Cell-Type-Specific and Site-Specific N-Glycosylation of Type I and Type II Human Tissue Plasminogen Activator

Raj B. Parekh,[‡] Raymond A. Dwek,[‡] Jerry R. Thomas,[‡] Ghislain Opdenakker,[§] and Thomas W. Rademacher*[,‡,∥]

Glycobiology Unit, Department of Biochemistry, University of Oxford, South Parks Road, Oxford OX1 3QU, U.K., and Rega Institute, University of Leuven, Minderbroedersstraat 10, B-3000 Leuven, Belgium

Arthur J. Wittwer, Susan C. Howard, Rickey Nelson, Ned R. Siegel, M. G. Jennings, Nikos K. Harakas, and Joseph Feder*

Department of Cell Culture and Biochemistry and Division of Biological Sciences, Monsanto Company, St. Louis, Missouri 63167

Received September 30, 1988; Revised Manuscript Received May 2, 1989

ABSTRACT: Tissue plasminogen activator (t-PA) is an important initiator of fibrinolysis. The t-PA polypeptide has four potential N-glycosylation sites of which three are occupied in type I (Asn-117, -184, and -448) and two in type II (Asn-117 and -448). In an effort to elucidate the factors controlling the expression of N-linked oligosaccharides on this polypeptide, we have used a combination of sequential exoglycosidase digestion, methylation analysis, and controlled acetolysis to determine the oligosaccharide structures at each of the N-glycosylation sites of type I and type II t-PA when isolated from a human colon fibroblast cell strain and from a Bowes melanoma cell line. Our results suggest the following: (i) type I and type II t-PA are N-glycosylated in an identical way at Asn-117 and Asn-448, when isolated from the same cell line; (ii) Asn-117 is predominantly associated with oligomannose-type structures in all cases; (iii) Asn-184 and Asn-448 are predominantly associated with complex-type structures when t-PA is isolated from fibroblast cells, but with both complex- and oligomannose-type structures when isolated from melanoma cells; (iv) fibroblast cell derived t-PA is associated with both neutral and sialylated oligosaccharides, while melanoma cell derived t-PA is also associated with sulfated oligosaccharides, which are located exclusively at Asn-448 of type II t-PA; (v) no complex-type structures occur in common between t-PA from the two cell lines. These results indicate that the t-PA glycoprotein is secreted by each cell line as a set of glycoforms, each glycoform being unique with respect to the nature and disposition of oligosaccharides on a common polypeptide. Further, the two cell lines express no glycoform in common, despite expressing the same t-PA polypeptide. The implications of these results for both the control of oligosaccharide processing in different cell lines and the genetic engineering of mammalian glycoproteins are discussed.

Tissue-type plasminogen activator (t-PA)[1] was discovered in 1947 (Astrup & Permin, 1947) and is now considered to have at least two major physiological functions. The first concerns its involvement in tissue histogenesis and remodeling during both normal development and neoplasia (Reich, 1975; Mullins & Rohrlich, 1983), and the second, its role as a physiologically important initiator of fibrinolysis (Bachmann & Kruithof, 1984), and it is this that has been most intensively studied. Dissolution of intravascular fibrin clots formed through the physiological or pathological activation of the blood coagulation system is a normal process essential for the maintenance of blood fluidity and is achieved by the proteolysis of fibrin by plasmin. The activation of plasminogen by t-PA is enhanced substantially more by the presence of fibrin than by fibrinogen, and this is probably due to the fact that both plasminogen and t-PA possess higher affinity binding sites for fibrin (Thorsen et al., 1972; Ranby, 1982; Zamarron et al., 1984; Bok & Mangel, 1985). Hence, t-PA is a powerful initiator of fibrinolysis with negligible fibrinogenolytic activity, and this unique property of t-PA makes it of potentially greater therapeutic value than urokinase or streptokinase in the initial treatment of thromboembolic disorders. These disorders (Verstraete et al., 1985), including coronary artery and cerebral artery thromboses, and deep vein thrombosis predisposing to pulmonary embolism, all involve vascular occlusion through the formation of fibrin clots.

The cDNA nucleotide and amino acid sequences of human t-PA have been determined and indicate homology with the "finger domain" of fibronectin, with mouse epidermal growth factor, with the Kringle structures found on some serum proteins, and with the chymotrypsin family of serine proteases (Pennica et al., 1983; Banyai et al., 1983). Although synthesized as a single polypeptide chain, the mature 528 amino acid sequence can be cleaved by plasmin to form a two-chain disulfide-linked molecule (Wallen et al., 1983) consisting of an A chain (amino acids 1–275) and a B chain (amino acids 276–528). It is a glycoprotein with four potential N-glycosylation sites (at Asn-117, -184, -218, and -448; Pohl et al., 1984), and like plasminogen (Hayes & Castellino, 1979), t-PA occurs naturally in two major variant forms. These are separable by chromatography on arginine-Sepharose (Ranby et al., 1982) or, more effectively, lysine–Sepharose (Einarsson et al., 1985) and are designated type I and type II t-PA. They do not appear to differ significantly in their polypeptide, but rather with respect to the degree of occupancy of the potential N-glycosylation sequons. In type I t-PA, Asn-117, -184, and -448 are occupied, but in type II t-PA N-linked oligosaccharides are found only at Asn-117 and -448 (Pohl et al., 1984). With the exception of a recent report by Pohl et al.

* Authors to whom correspondence should be addressed.
‡ University of Oxford.
§ University of Leuven.
∥ Author to whom reprint requests should be addressed.

[1] Abbreviations: t-PA, tissue-type plasminogen activator; Asn, asparagine; SDS-PAGE, sodium dodecyl sulfate–polyacrylamide gel electrophoresis; ELISA, enzyme-linked immunosorbent assay; hcf, human colon fibroblast; m, Bowes melanoma; DMEM, Dulbecco's modified Eagle's medium; HPLC, high-pressure liquid chromatography; mAU, milli absorbance units; Gal, galactose; Man, mannose; GlcNAc, *N*-acetylglucosamine; Fuc, fucose; GnT, *N*-acetylglucosaminyltransferase.

0006-2960/89/0428-7644$01.50/0

(1987) on the monosaccharide composition, endoglycosidase sensitivity, and methylation analysis of the glycopeptides derived from the three N-glycosylated sites of t-PA secreted by the Bowes melanoma cell line (Rijken & Collen, 1981), structural information on the carbohydrate structures present on t-PA is very limited, and this may explain, in part, the controversy that surrounds the effects of t-PA N-linked oligosaccharides on its fibrin-dependent activation of plasminogen. For example, when t-PA secreted by the Bowes melanoma cell line in the presence of tunicamycin (Rijken et al., 1985) or t-PA partially deglycosylated with Endo H (Little et al., 1984) was used, it was concluded that N-linked oligosaccharides did not affect the fibrin binding or fibrin-stimulated plasminogen activation of t-PA. In contrast, Opdenakker et al. (1986) found significant changes in the activity of t-PA after treating it with various exoglycosidases.

We have chosen to analyze the N-glycosylation of type I and type II t-PA secreted by the human Bowes melanoma cell line and CCD-18Co cells, a human colon fibroblast cell strain. Since t-PA is a glycoprotein with a well-defined range of measurable activities, it is a model system for studying the effects of N-glycosylation on the activity of a glycoprotein. Also, since the same human t-PA polypeptide can be isolated after expression in several cell types, an analysis of its N-glycosylation in each case can be used to probe the relative importance of cell type and polypeptide on N-glycosylation. Finally, the increasing therapeutic use of t-PA in the treatment of a variety of conditions involving acute thrombosis makes a knowledge of its N-glycosylation important per se. In this study we report a structural analysis of the N-linked oligosaccharides associated with each N-glycosylation site of type I and type II t-PA isolated from the Bowes human melanoma cell line and a human colon fibroblast cell strain (CCD-18Co). In subsequent reports we provide evidence that the differences in N-glycosylation between these two forms of t-PA reported here may be responsible for differences in their in vitro activities.

Materials and Methods

General. The following were obtained from the indicated sources: human colon derived CCD-18Co cells from the ATCC (CRL 1459), two-chain melanoma (m)-t-PA from American Diagnostica, Inc (product no. 110), lysine–Sepharose, fast S-Sepharose, and SDS gel low molecular weight standards (Pharmacia).

SDS–PAGE was performed by using Pharmacia's Phast System, employing their protocols for 10–15% gradient gels and silver staining. t-PA antigen was measured by a commercially available ELISA kit (American Diagnostica, Inc.). CCD-18Co cells were grown in DMEM containing 10% fetal calf serum. The cells were seeded onto Geli beads from roller bottle cultures and then maintained in a 12-L reactor to produce conditioned medium.

Purification of hcf-t-PA. Serum-containing conditioned medium from human colon fibroblast (hcf) cell culture was adjusted to pH 5.6 with acetic acid, and the plasminogen activator activity was purified by cation-exchange chromatography, essentially as described by Kruithof et al. (1985). This was followed by immunoaffinity chromatography using procedures described by Einarsson et al. (1985). A monoclonal antibody for this purpose (clone 79-7) was produced from mouse hybridoma cells by using hcf-t-PA, purified by the method of Rijken and Collen (1981), as the antigen. Following elution from the immunoaffinity resin, using 3 M KSCN, the preparation was further purified by HPLC gel filtration using a TSK 3000 SW column equilibrated with 1.6 M KSCN, 20 mM sodium phosphate buffer, and 0.01% Tween 80, pH 6.8. During this step, a partial separation from a higher molecular weight contaminant occurred, which presumably represented a t-PA–inhibitor complex. Final purification of the preparation with removal of this contaminant was achieved by chromatography on lysine–Sepharose using gradient elution (for the separation of type I from type II t-PA) or step elution (for the preparation of unfractionated hcf-t-PA) as described below. For some initial experiments, hcf-t-PA was purified from serum-free conditined medium following the procedure of Rijken and Collen (1981), except that HPLC gel filtration was used instead of chromatography on Sephadex G-150 (Harakas et al., 1988). In all cases, the resulting oligosaccharide and tryptic peptide profiles were similar, regardless of the method of purification.

Purification of m-t-PA. The two-chain m-t-PA obtained from American Diagnostica is derived from a Bowes melanoma line infected with mycoplasma. m-t-PA was therefore also purified from a mycoplasma-free Bowes melanoma line (Collen et al., 1982). The N-glycosylation of the m-t-PA derived from these two sources was determined (vide infra), and no difference was found (data not shown). The two-chain m-t-PA from American Diagnostica was therefore used for all the analyses reported here.

Lysine–Sepharose Chromatography. Type I and type II t-PA were separated by using lysine–Sepharose chromatography. A column of lysine–Sepharose (1.6 × 96 cm) was equilibrated at 4 °C with 5 volumes of 0.15 M KSCN, 120 mM NaCl, 2.7 mM KCl, and 10 mM phosphate buffer, pH 8.0, containing 0.01% Tween 20 (Pierce) and 0.01% NaN_3. The t-PA sample in 1 M NH_4HCO_3 was then applied to the column and washed with at least 40 mL of equilibration buffer. The column was then developed with a linear gradient (of total volume 500 mL), beginning with equilibration buffer and ending with an elution buffer containing 0.6 M arginine hydrochloride, 0.25 M KSCN, 120 mM NaCl, 2.7 mM KCl, and 10 mM phosphate buffer, pH 8.0, containing 0.01% Tween 20 and 0.01% NaN_3. Fractions (3 mL) were collected at 0.15 mL/min. The absorbance at 280 nm of the eluate was monitored continuously (Pharmacia dual-path monitor, UV-2), and the amidolytic activity (see below) and conductivity of the fractions were measured.

To remove significant amounts of contaminant from the unfractionated hcf-t-PA, t-PA in 1 M NH_4HCO_3 was applied to a similarly equilibrated column of lysine–Sepharose (0.9 × 30 cm), washed with equilibration buffer, and step eluted with the above elution buffer. The contaminant [presumably t-PA–inhibitor complex(es)] did not bind to the resin under these conditions. Recovery of t-PA amidolytic activity was over 90%. Pooled fractions were concentrated by using an Amicon pressure cell with a YM-10 membrane. The buffer was then changed to 1 M NH_4HCO_3 by using a small column of Sephadex G-25 (PD-10 column, Pharmacia). All intact t-PA for oligosaccharide analysis was rendered salt free by exhaustive flow dialysis against glass-distilled H_2O.

Amidolytic Assay for t-PA. A synthetic chromogenic substrate, S-2322 (H-D-Val-Gly-Arg-*o*-nitroanilide, Kabivitrum), was used to monitor column fractions for t-PA activity (Rijken & Collen, 1981). The assay was performed in 96-well microtitration plates (Immulon 1, Dynatech) with a total final volume of 100 μL. A 10-μL sample was added to a well followed by 90 μL of a reaction mixture composed of 1 part 2.5 mg/mL S-2322, 1 part 10× buffer (1 M NaCl, 1 mg/mL BSA, 200 mM Tris-HCl, and 0.1% Tween 80, pH 7.6), and 7 parts H_2O. The absorbance at 405 nm was monitored in

a plate reader (Molecular Devices). Activities were calculated from the linear absorbance increase with time between the range 0 and 100 mAU and were expressed as mAU/min.

Isolation and Identification of t-PA-Derived Glycopeptides. hcf-t-PA type I, hcf-t-PA type II, m-t-PA type I, and m-t-PA type II were separately dissolved in 1 M NH_4HCO_3 and lyophilized, and the residue was dissolved at a concentration of up to 1 mg/mL in buffer (0.1 M Tris-HCl, pH 8.15, 6 M guanidine hydrochloride, and 2 mM EDTA). After degassing under argon, sufficient 0.5 M dithiothreitol was added to yield a 5 mM final concentration, and the sample was incubated under argon for 1 h at 37 °C. Sufficient 0.5 M iodoacetate (in buffer) was then added to yield a 50 mM final concentration, and the incubation was continued for 1 h. The carboxymethylated protein was then desalted into 1 M NH_4HCO_3 by using a small column of Sephadex G-25 (PD-10 column, Pharmacia) and lyophilized. The residue was dissolved in 0.1 M NH_4HCO_3 to a concentration of about 0.5 mg/mL, and an amount of trypsin (Sigma, TPCK treated in 0.1 M NH_4HCO_3) equal to $^1/_{50}$ the weight of protein was added. Digestion was terminated by lyophilization after incubation for 10–12 h at room temperature. Lyophilized peptides were dissolved in 0.5–1 mL of 0.1% trifluoroacetic acid (TFA) and subjected to HPLC using a Nucleosil C-18, 5-μm, 100-A, 4.6 × 250 mm column (Macherey-Nagel, Inc.) at room temperature. A flow rate of 1 mL/min was maintained during gradient elution from 0% to 40% acetonitrile (0–120 min) and then from 40% to 90% acetonitrile (120–170 min). All HPLC elution solvents contained 0.1% TFA. The eluate was monitored at 215, 257, and 277 nm, and spectra of peaks were obtained by using an HP 1090A liquid chromatograph with photodiode array detector. Fractions of 1 mL (1 min) were collected. For oligosaccharide analysis the fractions eluting between 39 and 47 min were pooled for site Asn-448 glycopeptide, the fractions between 66 and 72 min for site Asn-184 glycopeptide, and the fractions between 72 and 76 min for site Asn-117 glycopeptide, and all were lyophilized.

The elution positions of the t-PA glycopeptides were established by preliminary experiments in which unfractionated two-chain hcf-t-PA and m-t-PA were individually reduced, carboxymethylated, separated into A and B chains, digested with trypsin, and subjected to reversed-phase HPLC as described above. The separation into A and B chains facilitates peptide identification and was accomplished by either reversed-phase HPLC or HPLC gel filtration. In the reversed-phase HPLC method, the reduced and carboxymethylated protein was dissolved in 0.1% TFA and applied to a Vydac C-4 column (214TP456, 5 μm, 300 A, 4.6 × 250 mm) equilibrated with 10% acetonitrile and 0.1% TFA. Elution was at room temperature and 1 mL/min flow rate with a linear gradient to 60% acetonitrile and 0.1% TFA at 100 min. As judged by SDS–PAGE, fractions between 47.0 and 52.5 min were pooled for the A chain and from 68.0 to 70.0 min for the B chain. Pooled fractions were evaporated to dryness in a Savant Speed-Vac. In the gel filtration method, the reduced and carboxymethylated protein was applied to a TSK-3000 SW column (2.15 × 30 cm) previously equilibrated with a 1.6 M KSCN and 20 mM sodium phosphate buffer, pH 6.8, with 0.01% Tween 80, and eluted at room temperature and 1 mL/min flow rate. SDS–PAGE revealed that the B chain eluted as a broad peak from 45 to 61 min, followed by the A chain at 62–69 min. The A and B chain fractions were concentrated, and the buffer was changed to 0.1 M ammonium bicarbonate. Equally pure preparations of the A and B chains were obtained by either method, as judged by the resulting tryptic peptide profiles.

Following reversed-phase HPLC, tryptic peptide fractions derived from the isolated A and B chains of hcf-t-PA and m-t-PA were analyzed to identify the elution positions of the peptides containing the potential N-glycosylation sites Asn-117, -184, -218 (A chain), and Asn-448 (B chain). Successive 2-min fractions across each chromatogram were analyzed for amino acid composition and glucosamine content, following acid hydrolysis. The results were then analyzed in light of the relative proportion and spectral properties of the peptides in each fraction and the published cDNA-derived amino acid sequence of m-t-PA. In this way it was possible to determine the elution positions of most of the expected tryptic peptides. For example, a fraction from the hcf-t-PA B chain was comprised of at least four resolved peptides peaks devoid of any aromatic UV absorbance. Amino acid analysis showed that glucosamine was present and gave the following relative composition: Asx (1.1), Thr (1.0), Ser (1.7), Glx (1.2), Leu (2.4), His (1.0), and Arg (1.0). It was therefore concluded that the expected tryptic peptide from site Asn-448, CTSQHLLNR, was present in this fraction [(carboxymethyl)cysteine was not determined]. The fractions in which potentially glycosylated peptides eluted were identical for both hcf-t-PA and m-t-PA, namely, 40–45 min for site Asn-448, 66–67 min for Asn-218, 68–70 and 76–77 min for Asn-184, and 73–75 min for Asn-117. Of these five elution ranges, the ones for Asn-448, Asn-117, and the 68–70-min range for Asn-184 were found also to contain glucosamine. No glucosamine was found elsewhere in the chromatographic fractions, indicating that Asn-218 is not N-glycosylated, that the Asn-184 peptide eluting at 76–77 min is not N-glycosylated, and that the glycopeptides from each N-glycosylated site elute in separate, nonoverlapping regions of the chromatogram.

To verify these results, an additional experiment was performed with hcf-t-PA only, in which peptides eluting in these regions were individually isolated, if necessary, by rechromatography on the reversed-phase column, and their sequence was determined. In the case of sites Asn-448, Asn-117, and glycosylated Asn-184, closely eluting peptides were combined prior to analysis on the basis of similar UV properties. Specifically, four peptides eluting between 42 and 44 min which lacked any aromatic UV absorbance were pooled for site Asn-448, two peptides eluting at about 74 min and having tryptophan-like spectra were combined for site Asn-117, and three peptides eluting in the 68–70-min region having tyrosine-like spectra were combined for glycosylated site Asn-184. N-Terminal sequence and composition analyses of these pools, and of the single peptides obtained for site Asn-218 and nonglycosylated Asn-184, gave compositions and sequences consistent with those expected for peptides containing these sites (Tables I and II). No signal due to Asn was found at the carbohydrate attachment site during sequencing of the Asn-448, Asn-117, and the 68–70-min Asn-184 peptides. This is consistent with glycosylation at these locations. Conversely, signals due to Asn-218 during sequencing of the 66–67-min peptide and due to Asn-184 during sequencing of the 76–77-min peptide, confirmed that these were not N-glycosylated. Unexpectedly, the site Asn-117 tryptic peptide was found to terminate with Tyr-126 instead of Arg-129. This may represent chymotryptic contamination of the tryptin used or an anomalous cleavage by trypsin (Jany et al., 1976).

When tryptic peptide fractions were pooled for oligosaccharide analysis, the range of elution times for each site was made wider than the minimum dictated by the elution times of the positively identified glycopeptides, so as to increase the likelihood of including any minor glycopeptides in each pool. Hence, fractions eluting at 39–47 min were pooled for site Asn-448, those at 66–72 min for site Asn-184, and those at 72–76 min for site Asn-117.

Amino Acid Composition and Sequence Analysis. For amino acid composition analysis, samples were subjected to

Table I: Amino Acid Analysis of the Tryptic Peptides That Contain the Potential N-Glycosylation Sites of hcf-t-PA[a]

	elution time (glycosylation site)				
amino acid	40–45 min (Asn-448)	66–67 min (Asn-218)	68–70 min (Asn-184)	73–75 min (Asn-117)	76–77 min (Asn-184)
cmCys	nd (1)	nd	nd (3)	nd (1)	nd (3)
Asx	1.0 (1)	1.0 (1)	3.2 (3)	2.2 (2)	3.1 (3)
Thr	0.9 (1)	0.9 (1)	1.0 (1)	3.0 (3)	1.0 (1)
Ser	1.1 (1)	1.0 (1)	5.6 (6)	4.3 (4)	5.1 (6)
Glx	1.2 (1)	2.0 (2)	2.3 (2)	3.5 (3)	2.6 (2)
Pro		1.0 (1)	0.7 (1)	1.3 (1)	1.1 (1)
Gly		1.9 (2)	3.4 (3)	2.5 (2)	3.3 (3)
Ala		2.8 (3)	2.3 (2)	4.7 (4)	2.1 (2)
Val		0.9 (1)			
Met					
Ile					
Leu	2.0 (2)	1.8 (2)		1.2 (1)	
Tyr		0.7 (1)	2.0 (3)	+[b] (1)	2.3 (3)
Phe			1.9 (2)		2.1 (2)
Trp[c]	–	–	–	+ (2)	–
His	1.0 (1)				
Lys		+[d] (1)		1.0 (1)	
Arg	1.0 (1)		1.0 (1)		1.0 (1)
glucosamine[e]	+	–	+	+	–

[a] Amino acid values are given as molar ratios normalized to either Lys or Arg. Theoretical compositions based on the expected tryptic peptides containing each glycosylation site (Pennica et al., 1983) are given in parentheses. The Asn-117 peptide was found to terminate with Tyr-126 instead of Arg-129, so this was used to determine theoretical composition in this case. Results are presented without correction for destruction or incomplete liberations during acid hydrolysis. Values lower than 0.3 are omitted. (Carboxymethyl)cysteine (cmCys) was not determined (nd). [b] Tyr was not quantitated because of its close elution with glucosamine. [c] Trp was indicated by the presence (+) or absence (–) of its characteristic UV spectrum. [d] Lys was not quantitated due to integrator error, and in this case composition was normalized to Asx. [e] Glucosamine was indicated by the presence (+) or absence (–) of a broad peak eluting in the Tyr region during amino acid analysis.

Table II: Sequence Analysis of the Tryptic Peptides from hcf-t-PA That Contain Potential N-Glycosylation Sites[a]

	elution time (glycosylation site)				
cycle	40–45 min (Asn-448)	66–67 min (Asn-218)	68–70 min (Asn-184)	73–75 min (Asn-117)	76–77 min (Asn-184)
1	Cys (–)	Val (968)	Tyr (876)	Gly (2471)	Tyr (1363)
2	Thr (1158)	Tyr (932)	Ser (–)	Thr (2154)	Ser (370)
3	Ser (781)	Thr (726)	Ser (–)	Trp (1684)	Ser (289)
4	Glu (1654)	Ala (972)	Glu (315)	Ser (648)	Glu (678)
5	His (336)	Glu (843)	Phe (396)	Thr (1213)	Phe (1019)
6	Leu (1002)	Asn (657)	Cys (–)	Ala (3130)	Cys (–)
7	Leu (1093)	Pro (761)	Ser (–)	Glu (2374)	Ser (148)
8	*b* (–)	Ser (258)	Thr (–)	Ser (1002)	Thr (222)
9	Arg (170)	Ala (560)	Pro (181)	Gly (982)	Pro (373)
10		Glu (479)	Ala (158)	Ala (1296)	Ala (317)
11		Ala (400)	Cys (–)	Glu (1146)	Cys (–)
12		Leu (339)	Ser (–)	Cys (–)	Ser (152)
13		Gly (275)	Glu (62)	Thr (561)	Glu (254)
14		Leu (189)	Gly (80)	Asn (862)	Gly (132)
15		Glu (208)	Asn (75)	Trp (373)	Asn (171)
16		Lys (147)	Ser (–)	*b* (–)	Ser (39)
17			Asp (39)	Ser (202)	Asp (142)
18			Cys (–)	Ser (215)	Cys (–)
19			Tyr (32)	Ala (135)	Tyr (36)
20			Phe (47)	Leu (77)	Phe (27)
21			Gly (28)	Ala (107)	Gly (64)
22			*b* (–)	Glu (102)	Asn (82)
23			Gly (18)	*c* (–)	Gly (7)
24			Ser (–)	Pro (64)	Ser (9)
25			Ala (16)	Tyr (–)	Ala (22)
26			Tyr (18)		Tyr (8)
27			*d* (–)		*d* (–)

[a] Identity of the major amino acids liberated at each cycle is indicated along with its recovery in picomoles. Cys was identified as the carboxymethyl derivative but was not quantitated. Other amino acids identified but not quantitated are indicated (–). [b] No amino acid detected at this cycle. Asn was anticipated on the basis of the known primary amino acid sequence of t-PA (Pennica et al., 1983). [c] No amino acid detected at this cycle. Lys was expected (Pennica et al., 1983). [d] No amino acid detected at this cycle. Arg was expected (Pennica et al., 1983).

vapor-phase acid hydrolysis (6 N HCl, Pierce) in evacuated, sealed hydrolysis vials for 24 h at 110 °C. Phenol (1%) was added to improve yields of tyrosine, but no effort was made to minimize the oxidative destruction of cysteine and methionine. Following hydrolysis, the excess HCl was removed by evaporation and the samples were reconstituted in a sample dilution buffer, 0.2 N sodium citrate, pH 2.2 (Beckman), and loaded onto the Beckman System 6300 high performance analyzer, which employs a postcolumn ninhydrin-based detection system. Comparisons to external standard mixtures of amino acids provided the basis for quantitation.

Automated Edman degradation was used to determine NH_2-terminal peptide sequences. An Applied Biosystems Inc. Model 470A gas-phase sequencer (Foster City, California) was employed for the degradations (Hunkapiller et al., 1983). The respective PTH-amino acid derivatives were identified by reversed-phase HPLC using an Applied Biosystems Inc. Model 120A PTH analyzer fitted with a Brownlee 2.1-mm (i.d.) PTH-C18 column.

Release, Labeling, and Isolation of Asparagine-Linked Oligosaccharides. Between 3 and 15 nmol of t-PA glycoprotein, or glycopeptides derived from t-PA, was cryogenically

dried over activated charcoal at −196 °C (<10^6 bar). The samples were suspended in 200–300 μL of freshly distilled anhydrous hydrazine (toluene/CaO, 25 °C, 10 Torr) under an anhydrous argon atmosphere. The temperature was raised 17 °C/h from 30 to 85 °C and then maintained at 85 °C for a further 12 h. The hydrazine was removed by evaporation under reduced pressure (<10^{-4} bar) at 25 °C followed by repeated (5×) flash evaporation from anhydrous toluene (thiophene and carbonyl free). The hyrazinolysates were N-acetylated by the addition of excess (5× over amino groups) acetic anhydride (0.5 M) in saturated $NaHCO_3$ at 4 °C for 10 min. The temperature was then raised to 25 °C, a second aliquot of acetic anhydride added, and the reaction allowed to proceed for a further 50 min. Following N-acetylation, the samples were applied to a column of Dowex AG50X 12 (H^+), eluted with water and evaporated to dryness (27 °C). The desalted samples were dissolved in water and applied to Whatman 3MM chromatography paper. Descending paper chromatography (27 °C, 70% RH) was subsequently performed with 1-butanol/ethanol/water (4:1:1 v/v) (solvent I). After 48 h the first 5 cm measured from the origin was eluted with water, flash-evaporated to dryness (27 °C), redissolved in a 5× molar excess of 1 mM copper(II) acetate, and incubated at room temperature for 45 min. After passage through a tandem column of Chelex 100 (Na^+)/Dowex AG50X 12-(H^+), the oligosaccharides were flash-evaporated to dryness (27 °C) and reduced with a 5-fold molar excess of 6 mM NaB^3H_4 (70.2 Ci/mmol, obtained from New England Nuclear Co.) in 50 mM NaOH adjusted to pH 11 with saturated boric acid (30 °C, 4 h). An equivalent volume of 1 M $NaBD_4$ in NaOH/boric acid, pH 11, was then added and the incubation continued for a further 2 h. The mixture was then acidified (pH 4–5) with 1 M acetic acid and applied to a column of Dowex AG50X 12 (H^+), eluted with water, evaporated to dryness (27 °C), and flash-evaporated (27 °C) from methanol (5×). The samples were then applied to Whatman 3MM chromatography paper and subjected to descending paper chromatography for 2 days using solvent I.

Radiochromatogram scanning was performed with an LB230 Berthold radiochromatogram scanner. The radioactivity remaining at the origin was subsequently eluted with water. The isolated oligosaccharides were subjected to high-voltage paper electrophoresis in pyridine/acetic acid/water (pH 5.4, Whatman 3MM, 80 V/cm) in order to determine the relative proportions of neutral and acidic components [lactitol (L) and 3′(6′)-sialyllactitol (SL) were used as standards]. An aliquot of the reduced (^3H-labeled) oligosaccharides were also subjected to exhaustive neuraminidase digestion, and the products were separated by high-voltage paper electrophoresis. All radioactivity remaining at the origin following neuraminidase digestion was recovered by elution with water and desalted by using a tandem column of Chelex 100 (Na^+)/Dowex AG50X 12 (H^+)/AG3X 4A (OH^-)/QAE-Sephadex A-25, and the eluate and washings were evaporated to dryness, resuspended in 175 μL of a 2 mg/mL partial dextran hydrolysate, and applied to a Bio-Gel P-4 (~400 mesh) gel permeation chromatography column (1.5 × 200 cm). The eluant was monitored for radioactivity by using an LB503 Berthold HPLC radioactivity monitor, and for refractive index by using an Erma ERC 7510 refractometer. Analog signals from the monitors were digitized with Nelson Analytical ADC interfaces. The digital values were collected and analyzed on Hewlett-Packard 9836 C computers. The P-4 chromatograms show radioactivity (vertical axis) plotted against retention time. The numerical superscripts refer to the elution position of the glucose oligomers in glucose units as detected simultaneously by the refractive index monitor (data not shown). V_0 is the void position. Sample elution positions (in glucose units) were calculated by cubic spline interpolation between the internal standard glucose oligomer positions.

Enzymes. Jack bean β-galactosidase, β-*N*-acetylhexosaminidase, and α-mannosidase were purified from jack bean meal (Sigma) according to Li and Li (1972). All three enzymes were then finally purified by free-boundary zonal electrophoresis. Enzyme solution (in a buffer of pH identical with its isoelectric point) was eluted into a bed of ethanolized microcrystalline cellulose equilibrated in the same buffer (19 °C). A voltage (280 V) was applied by using Ag/AgCl (KCl) electrodes for a time sufficient to remove all contaminating exoglycosidase activities, and the enzyme was then eluted. After this purification step, the β-galactosidase will hydrolyze β1→4- but not β1→3-linked nonreducing terminal galactose residues (unpublished results). The α1→2 specific mannosidase from *Aspergillus phoenicis* was purified from culture supernatant according to Ichishima et al. (1981) and finally purified by free-boundary zonal electrophoresis, as described above. *Streptococcus pneumoniae* β-galactosidase and β-*N*-acetylhexosaminidase were first purified from culture supernatant according to Glasgow et al. (1977) and traces of contaminatng exoglycosidase activity removed by repeated anion-exchange chromatography. All other enzymes were obtained from the following sources: bovine epididymis α-fucosidase (Sigma); *Arthrobacter ureafaciens* neuraminidase (Boehringer-Mannheim); *Escherichia coli* alkaline phosphatase (Sigma); *Achatina fulica* β-mannosidase (Seikagaku Kogyo Co., Tokyo); Newcastle disease virus neuraminidase (Delvax, Delft, Holland). All exoglycosidases other than *E. coli* alkaline phosphatase and Newcastle disease virus neuraminidase were exhaustively checked for the presence of contaminating exo- and endoglycosidase activities against a panel of standard, reduced oligosaccharides (vide infra). All digestions, to check for contaminating activity were perfrmed at 37 °C for 18 h under toluene, and under conditions designed to increase detection of the putative contaminant. Products were then analyzed by Bio-Gel P-4 gel permeation chromatography or high-voltage paper electrophoresis. In this way contaminating activities of 1 part in 10^4 can easily be detected. All exoglycosidases were rendered free of contamination (at this level) prior to use.

Exoglycosidase Digestions. Digestion of ^3H-labeled oligosaccharides (~2×10^5 cpm) with exoglycosidases of defined specificities (Kobata, 1979) was carried out under the following conditions: jack bean β-galactosidase, 20 μL of 6 units/mL in 0.05 M sodium citrate, pH 3.5; jack bean β-*N*-acetylhexosaminidase, 20 μL of 10 units/mL in 0.1 M citrate–phosphate, pH 4.0; jack bean α-mannosidase, 20 μL of 50 units/mL in 0.1 M sodium acetate, pH 4.5; for use of jack bean α-mannosidase under arm-specific conditions (Kobata, 1984) under which R→Manα1→6(Manα1→3)Manβ1→4GlcNAcβ1→4GlcNAc$_{OT}$ but not Manα1→6(R→Manα1→3)Manβ1→4GlcNAcβ1→4GlcNAc$_{OT}$ is susceptible, 5×10^5 cpm of oligosaccharide was incubated with 30 μL of 10 units/mL jack bean α-mannosidase in 0.1 M sodium acetate, pH 4.5; *S. pneumoniae* β-galactosidase, 20 μL of 0.2 unit/mL in 0.1 M citrate–phosphate, pH 6.0; *S. pneumoniae* β-*N*-acetylhexosaminidase, 20 μL of 0.1 unit/mL in 0.1 M citrate–phosphate, pH 6.0; *A. phoenicis* α-mannosidase, 20 μL of 20 μg/mL in 0.1 M sodium acetate, pH 5.0; bovine epididymis α-fucosidase, 20 μL of 1 unit/mL in 0.2 M citrate–phosphate, pH 6.0; *A. ureafaciens* neuraminidase, 20 μL of 10 units/mL in 0.1 M sodium acetate, pH 5.0; Newcastle disease virus neuraminidase, 30 μL containing 1×10^8 EID_{50} in 0.1 M sodium acetate; *A. fulica* β-mannosidase, 20 μL of 0.2 unit/mL in 0.5 M sodium citrate, pH 4.0; *E. coli* alkaline phosphatase, 30 μL of 6 units/mL in 0.05 M Tris buffer, pH

8.0. Where applicable, 1 unit of exoglycosidase is defined as the amount of enzyme which, in control experiments, releases 1 μmol of 4-nitrophenol, from the repective 4-nitrophenyl glycoside, per minute at 37 °C. All incubations were carried out for 18 h at 37 °C under toluene and were terminated by heating to 100 °C for 2 min (except incubations involving neuraminidase, which were terminated by subjecting the entire incubation mixture to high-voltage paper electrophoresis, as described above).

Desulfation by Methanolysis. Reduced desialylated oligosaccharide was lyophilized, suspended in 200 μL of 0.05 M HCl in anhydrous methanol, incubated in a sealed tube under an atmosphere of anhydrous argon at 25 °C for 15 h, dried under vacuum, and then re-N-acetylated (vide infra).

Acetolysis. Desialylated oligosaccharide fractions [obtained after Bio-Gel P-4 (−400 mesh) gel permeation chromatography] were exhaustively digested with bovine epididymis α-fucosidase prior to acetolysis. Acetolysis was performed essentially as described by Natsuka et al. (1987), with the following modifications. Acetolysis of O-acetylated oligosaccharides was performed at 40 °C for 1.5 h. Under these conditions, a time course study on the oligomannose structure Man-9 [standard oligosaccharide x (vide infra)] was found to achieve ~30% hydrolysis of Manα1→6 bonds with minimal hydrolysis of other bonds in the Man-9 oligosaccharide. For complex-type oligosaccharides, under these conditions [standard oligosaccharides xiii and defucosylated xx (vide infra)], completely selective cleavage of the Manα1→6 bond could not be achieved and product analysis of the fragments generated was necessary [see Elices and Goldstein (1989)]. Following acetolysis, sulfate anions were separated from oligosaccharides by passage of the acetolysis mixture through an AG3X 4A (acetate) column (of bed volume 400 μL) equilibrated and washed in 70% methanol (v/v). Eluant and washings were pooled and flash-evaporated to dryness, and oligosaccharides were de-O-acetylated as described by Bischoff et al. (1986). Following de-O-acetylation, the oligosaccharide mixture was subjected to Bio-Gel P-4 (~400 mesh) gel permeation chromatography, as already described, and only the intact starting material and the product retaining the original reduced terminus were detected.

Methylation Analysis. Samples were permethylated according to a modification of the method of Ciucanu and Kerek (1987). Reduced oligosaccharides (dextran free) were dissolved in 50 μL of dimethyl sulfoxide, and 50 μL of 120 mg/mL colloidal solution of NaOH in dimethyl sulfoxide was added and the mixture incubated at room temperature with stirring for 30 min. Three aliquots of methyl iodide (10 μL) were added with 10 min of stirring after each addition. The partially methylated oligosaccharides were extracted by the addition of 0.3 mL of chloroform and 1 mL of a 100 mg/mL aqueous solution of sodium thiosulfate, with thorough mixing. The aqueous phase was discarded and the organic phase extracted 4× with 4 × 1 mL of water. The organic phase was evaporated to dryness under reduced pressure and 0.1 mL of 93% acetic acid/0.25 N sulfuric acid added (80 °C for 2.5 h). The sample was then passaged through an AG3X 4A (acetate) column (bed volume 0.5 mL) and the column washed five times with 0.5 mL of 50% methanol (v/v). After drying, the sample was reduced with 200 μL of a 10 mg/mL solution of $NaBO_4$. The sample was then neutralized with acetic acid and borate removed by flash evaporation (5×) from acidified methanol (0.3 mL). Residual acetic acid was removed by flash evaporatioin (3×) from methanol. Acetic anhydride (0.25 mL) was then added and the sample incubated at 85 °C for 3 h. The acetic anhydride was removed by evaporation under vacuum and the partially methylated alditol acetates (PMAA) extracted by the addition of 0.5 mL of dichloromethane and 1 mL of water. After thorough mixing the aqueous phase was discarded. Analysis of the PMAAs was performed on a Hewlett-Packard 5996C GLC-MS system fitted with on-column injection and flame-ionization detection. Separation was by capillary GLC on a bonded-phase CP-Sil 8 CB column (0.32 mm × 25 m, Chrompack, London, U.K.) with helium as the carrier gas. Direct on-column injection was employed with a temperature program of 90 °C (held for 1 min), followed by a linear increase to 140 °C at 30 °C/min, and then to 250 °C at 5 °C/min. Data were collected by selected-ion monitoring, and identification of each PMAA was based on retention time and mass spectrum by comparison with synthetic reference compounds, or published data.

Standard Oligosaccharides. Standard oligosaccharides were prepared from glycoproteins by hydrazinolysis with subsequent reduction with NaB^3H_4 (OT), and where appropriate, products were generated from standard oligosaccharides by exoglycosidase digestion (as stated below).

(i) (Galβ1→4GlcNAcβ1→2)(Galβ1→4GlcNAcβ1→6)-Manα1→6[Galβ1→4GlcNAcβ1→2(Galβ1→4GlcNAcβ1→-4)Manα1→3]Manβ1→4GlcNAcβ1→$4GlcNAc_{OT}$ was prepared from human α-1-acid glycoprotein.

(ii) Galβ1→4GlcNAcβ1→3Galβ1→4GlcNAcβ1→-2Manα1→6(Galβ1→4GlcNAcβ1→2Manα1→3)Manβ1→-4GlcNAcβ1→$4GlcNAc_{OT}$ was prepared from human lactoferrin.

(iii) Galβ1→4GlcNAcβ1→2Manα1→6[Galβ1→-4GlcNAcβ1→4(Galβ1→4GlcNAcβ1→2)Manα1→3]-Manβ1→4GlcNAcβ1→$4GlcNAc_{OT}$ was prepared from bovine fetuin.

(iv) (Galβ1→4GlcNAcβ1→2)(Galβ1→4GlcNAcβ1→6)-Manα1→6(Galβ1→4GlcNAcβ1→2Manα1→3)Manβ1→-4GlcNAcβ1→$4GlcNAc_{OT}$ was prepared from rat thymocyte Thy-1.

(v) GlcNAcβ1→2Manα1→6[GlcNAcβ1→4(GlcNAcβ1→-2)Manα1→3]Manβ1→4GlcNAcβ1→$4GlcNAc_{OT}$ was prepared from iii by treatment with jack bean β-galactosidase.

(vi) (GlcNAcβ1→2)(GlcNAcβ1→6)Manα1→6-(GlcNAcβ1→2Manα1→3)Manβ1→4GlcNAcβ1→-4GlcNAc$_{OT}$ was prepared by β-galactosidase treatment of iv.

(vii) NeuNAcα2→6Galβ1→4GlcNAcβ1→2Manα1→6-(NeuNAcα2→6Galβ1→4GlcNAcβ1→2Manα1→3)-Manβ1→4GlcNAcβ1→$4GlcNAc_{OT}$ was prepared from human serum IgG.

(viii) Galα1→3Galβ1→4GlcNAcβ1→2Manα1→6-(Galβ1→4GlcNAcβ1→2Manα1→3)Manβ1→4GlcNAcβ1→-4GlcNAc$_{OT}$ was prepared from rat thymocyte Thy-1.

(ix) Galβ1→3GlcNAcβ1→2Manα1→6(Galβ1→-3GlcNAcβ1→2Manα1→3)Manβ1→4GlcNAcβ1→-4GlcNAc$_{OT}$ was prepared from bovine prothrombin.

(x) (Manα1→2Manα1→6)(Manα1→2Manα1→3)-Manα1→6(Manα1→2Manα1→2Manα1→3)Manβ1-4GlcNAcβ1→$4GlcNAc_{OT}$ was prepared from soybean agglutinin.

(xi) Manα1→6(Manα1→3)Manα1→6(Manα1→3)-Manβ1→4GlcNAcβ1→$4GlcNAc_{OT}$ was prepared from bovine ribonuclease B.

(xii) Manα1→6(Manα1→3)(Xylβ1→2)Manβ1→-4GlcNAcβ1→4(Fucα1→3)GlcNAc$_{OT}$ was prepared from *Erythrina cristagalli*.

(xiii) Galβ1→4GlcNAcβ1→2Manα1→6(Galβ1→-4GlcNAcβ1→2Manα1→3)Manβ1→4GlcNAcβ1→-4GlcNAc$_{OT}$ was prepared from human serum transferrin.

(xiv) Galβ1→4GlcNAcβ1→2Manα1→6(Galβ1→-4GlcNAcβ1→2Manα1→3)Manβ1→4GlcNAcβ1→4-(Fucα1→6)GlcNAc$_{OT}$ was prepared from human serum IgG.

(xv) Galβ1→4GlcNAcβ1→2Manα1→6(Manα1→3)-Manβ1→4GlcNAcβ1→4(Fucα1→6)GlcNAc$_{OT}$ was prepared

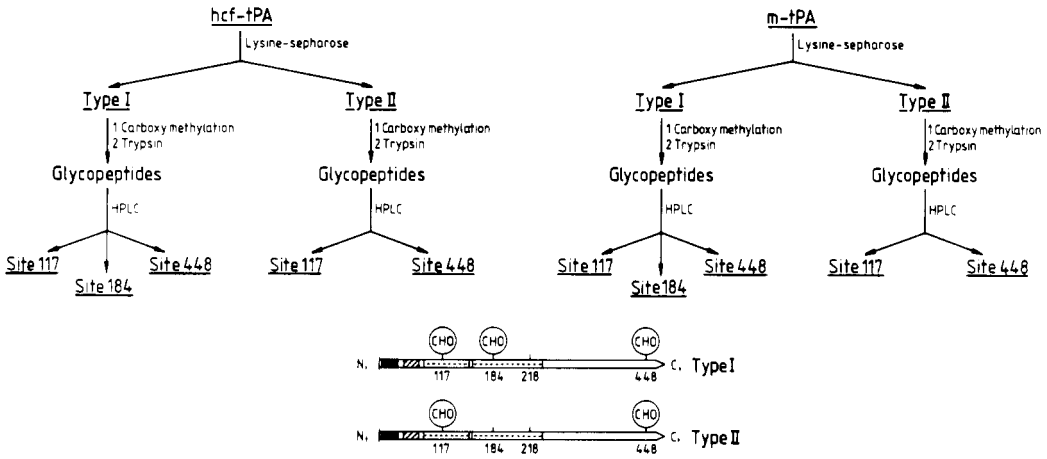

FIGURE 1: Strategy of fractionation of t-PA and its glycopeptides. The N-linked oligosaccharides were analyzed from all samples that are underlined. Tryptic glycopeptide fractions containing N-glycosylation sites Asn-117, Asn-184, and Asn-448 are designated by the number of the appropriate Asn residue. Also shown is a schematic representation of the t-PA polypeptide. Potential N-glycosylation sites (at Asn-117, Asn-184, Asn-218, and Asn-448) are indicated, together with the sites known to be occupied in type I and type II t-PA. Areas of amino acid homology with the "finger domain" of fibronectin [residues 6–43 (solid bar)], with EGF [residues 56–84 (hatched bar)], and with the Kringle domain [residues 92–173 (KI) and 180–261 (K2) (bar with dashed line)] are as shown.

by exoglycosidase digestion of monosialylated xiv.

(xvi) Manα1→6(Galβ1→4GlcNAcβ1→2Manα1→3)-Manβ1→4GlcNAcβ1→4(Fucα1→6)GlcNAc$_{OT}$ was prepared by exoglycosidase digestion of monosialylated xiv.

(xvii) GlcNAcβ1→2Manα1→6(GlcNAcβ1→2Manα1→-3)β1→4GlcNAcβ1→4GlcNAc$_{OT}$ was prepared from xiii by β-galactosidase treatment.

(xviii) GlcNAcβ1→2Manα1→6(GlcNAcβ1→2Manα1→-3)(GlcNAcβ1→4)Manβ1→4GlcNAcβ1→4(Fucα1→6)-GlcNAc$_{OT}$ was prepared from human serum IgG.

(xix) Manα1→6(Manα1→3)(GlcNAcβ1→4)Manβ1→-4GlcNAcβ1→4GlcNAc$_{OT}$ was prepared by digestion of ovomucoid oligosaccharides eluting at ~10.5 glucose units (g.u.) with *S. pneumoniae* β-*N*-acetylhexosaminidase.

(xx) Manα1→6(Manα1→3)Manβ1→4GlcNAcβ1→4-(Fucα1→6)GlcNAc$_{OT}$ was obtained by β-galactosidase and jack bean β-*N*-acetylhexosaminidase digestion of vii.

(xxi) Manβ1→4GlcNAcβ1→4(Fucα1→6)GlcNAc$_{OT}$ was obtained by jack bean α-mannosidase digestion of xx.

(xxii) GlcNAcβ1→4(Fucα1→6)GlcNAc$_{OT}$ was obtained by *A. fulica* β-mannosidase digestion of xxi.

(xxiii) Fucα1→6GlcNAc$_{OT}$ was obtained by jack bean β-*N*-acetylhexosaminidase digestion of xxii.

(xxiv) GlcNAcβ1→4GlcNAc$_{OT}$ was obtained by α-fucosidase treatment of xxii.

(xxv) GlcNAc$_{OT}$ was obtained by reduction of *N*-acetylglucosamine.

RESULTS

Strategy of the Analysis. The scheme for the fractionation of hcf-t-PA and m-t-PA and for isolation of glycopeptide fractions from each of the type I and type II forms is shown in Figure 1. After the fractions containing the glycopeptides from a particular N-glycosylation site were pooled, the attached oligosaccharides were released and subjected to structural analysis. At the end of the analysis, the sum of the structures from the glycopeptides was compared to the structures from the intact glycopeptides, so as to assess the accuracy of the analysis.

Separation of m-t-PA and hcf-t-PA into Type I and Type II. hcf-t-PA was purified from the conditioned medium of CCD-18Co cells by cation-exchange chromatography, anti-t-PA monoclonal antibody affinity chromaography, and size exclusion HPLC. Commercially obtained two-chain m-t-PA and purified hcf-t-PA were subjected to chromatography on lysine–Sepharose with elution by an arginine gradient (Figure 2). In each case two peaks of protein, each of which had t-PA amidolytic activity, were detected. In accordance with the observation of others, the first peak was designated as type I and the second peak as type II (Ranby et al., 1982; Pohl et al., 1984; Rijken et al., 1985). Subsequent analysis confirmed these assignments (see below). The high degree of separation between the two forms seen here is probably due to the greater column length employed, as noted by Einarsson et al. (1985).

Compared to the m-t-PA (Figure 2b), the first hcf-t-PA peak from lysine–Sepharose chromatography appeared to be broader, with a prominent shoulder around fractions 120–130 (Figure 2a). In quantitative terms, the first peak (fractions 110–152) comprised somewhat more of the eluted amidolytic activity for the hcf-t-PA (62%) than for the m-t-PA (52%). The central fractions from each peak were pooled for further analysis, as indicated.

SDS–PAGE of the unfractionated, type I, and type II hcf-t-PA and m-t-PA preparations showed not only an absence of contaminating polypeptide, but also the expected molecular weight difference between them, with type I being slightly larger than type II. As expected, a doublet is observed in the unfractionated t-PA (Figure 2d). Under reducing conditions (Figure 2c) the t-PA samples were found to be essentially all in the two-chain form. This was expected, since the hcf-t-PA was purified from serum-containing medium without the addition of any protease inhibitor (Rijken & Collen, 1981) and the m-t-PA used for these studies was purchased in the two-chain form.

Isolation of Glycopeptides from Type I and Type II hcf- and m-t-PA. Reduced and carboxymethylated samples of type I and type II t-PA from each cell type were digested with trypsin and the resulting peptides separated by reversed-phase HPLC. The four HPLC elution profiles (Figure 3a–d), while generally similar, showed important differences.

Preliminary experiments using unfractionated hcf- and m-t-PA established the elution positions of the tryptic peptides derived from each potential N-glycosylation site. The reproducible naure of the HPLC separation allowed identification of the peptides of interest in the type I and type II profiles shown in Figure 3, by analogy to this previous work. The prominent peptide at 76–77 min in the digests of type II t-PA (Figure 3c,d) was identified as the nonglycosylated tryptic peptide containing the potential N-glycosylation site Asn-184. As expected, the peptide at 76–77 min was not present in the digests of type I t-PA (Figure 3a,b). Instead, several peptides

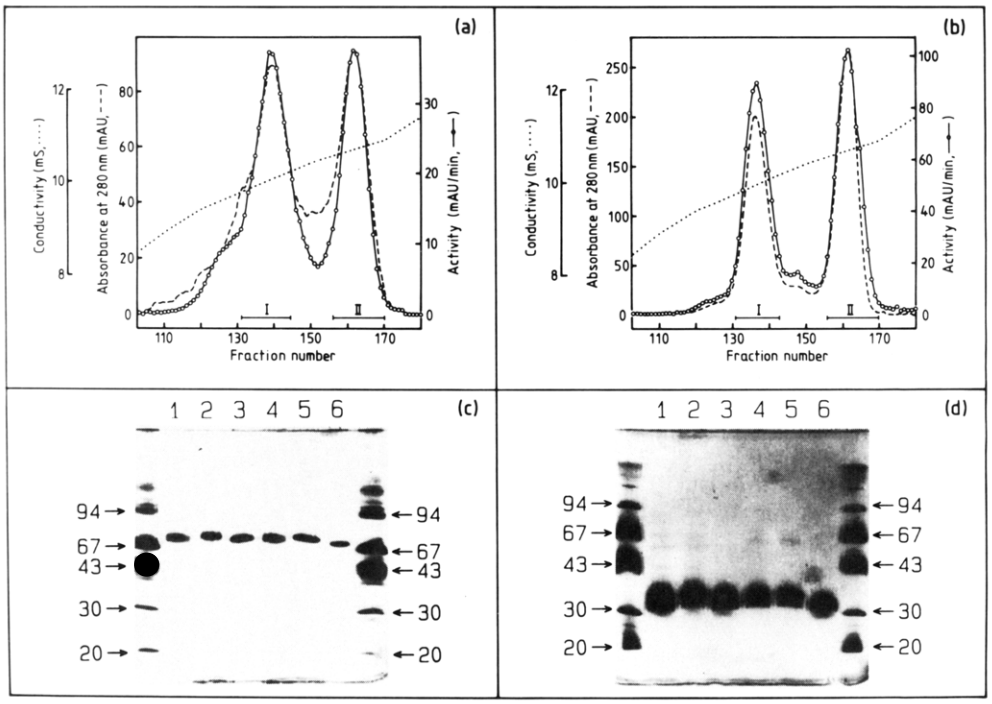

FIGURE 2: Fractionation of hcf-t-PA (a) and of m-t-PA (b) into type I and type II by lysine–Sepharose chromatography. In the case of hcf-tPA, about 2 mg of t-PA was applied to the column, and fractions 131–145 were pooled for type I and fractions 156–170 for type II. In the case of m-t-PA, about 4 mg of two-chain t-PA was applied, and fractions 131–143 were pooled for type I and fractions 156–170 for type II. SDS–PAGE of hcf-t-PA, m-t-PA, and their type I and II forms was prepared by using 100 ng (approximately) of each t-PA under both nonreducing (c) and reducing (d) conditions. Identity of samples is as follows: lane 1, unfractionated hcf-t-PA; lane 2, type I hcf-t-PA; lane 3, type II hcf-t-PA; lane 4, unfractionated m-t-PA; lane 5, type I m-t-PA; lane 6, type II m-t-PA. Molecular weight standards were applied to the outermost lanes and are, as indicated, phosphorylase *b* (94K), bovine serum albumin (67K), ovalbumin (43K), carbonic anhydrase (30K), and soybean trypsin inhibitor (20K).

were apparent in the region 68–70 min which, in turn, were absent from the digests of type II t-PA. These peptides were identified as glycopeptides derived from Asn-184. These results confirmed the assignment of the two lysine–Sepharose fractions as type I (glycosylated at Asn-184) and type II (not glycosylated at Asn-184). Additional "families" of glycopeptides containing the glycosylation sites Asn-117 (73–75 min) and Asn-448 (40–45 min) were found in the tryptic digests of both type I and type II t-PA (Figure 3a–d). Finally, a nonglycosylated tryptic peptide containing site Asn-218 was found in each profile in the 66–67-min region. This suggests that both hcf-t-PA and m-t-PA lack glycosylation at Asn-218, in agreement with previous results for m-t-PA (Pohl et al., 1984).

It is of interest that the glycosylated peptides for a particular site were found as families of closely eluting peaks. A split peak was found for the peptide from site 117, at least three peaks for site 184, and four or more for site 448. This is presumably due to the heterogeneity of oligosaccharide structures at each of these three sites as seen in subsequent glycosylation analyses (see below) and is similar to results obtained with rat Thy-1 (Parekh et al., 1987).

One further difference in peptide was evident. A significant proportion (60–70%) of native two-chain hcf-t-PA was found to be lacking in the amino acid residue Arg-275. The des-Arg tryptic peptide (QYSQPQF) was identified by sequence and composition analysis as eluting in the 59–60-min region and is prominent in the hcf-t-PA profiles (Figure 3a,c). This peptide is absent in the m-t-PA digest. Instead, the expected tryptic peptide (QYSQPQFR) was identified as eluting in the 52–53-min region and is readily apparent in the m-t-PA profiles (Figure 3b,d). The simplest explanation for these results is that an enzyme with carboxypeptidase B like specificity removes Arg-275 from two-chain hcf-t-PA. It is not known whether this occurs during the cell culture process or during purification, or whether it affects t-PA activity. It should be noted, however, that the amount of des-Arg peptide is essentially the same for the two types of hcf-t-PA.

Structural Analysis of the N-Linked Oligosaccharides Released from Unfractionated hcf-t-PA. An aliquot of the mixture of reduced oligosaccharides isolated from unfractionated hcf-t-PA was first subjected to high-voltage paper electrophoresis, and the resulting profile is shown in Figure 4a. The relative amount of neutral (N) and acidic (A) components were determined by recovery of radioactivity from paper (Table III). Treatment prior to electrophoresis of an aliquot of this mixture with the Newcastle disease virus neuraminidase caused no change in the resulting radioelectrophoretogram (data not shown), but prior treatment with the neuraminidase from *A. ureafaciens* caused conversion of *all* acidic oligosaccharides to neutral (Figure 4a, inset). Since Newcastle disease virus neuraminidase will only hydrolyze $\alpha 2 \rightarrow 3$-linked sialic acid (Paulson et al., 1982), and that from *A. ureafaciens*, both $\alpha 2 \rightarrow 3$- and $\alpha 2 \rightarrow 6$-linked sialic acid (Kobata, 1979), this result indicates that an $\alpha 2 \rightarrow 6$-linked sialic acid, and only this, is responsible for the acidic nature of the hcf-t-PA-derived acidic N-linked oligosaccharides. The oligosaccharides obtained after neuraminidase digestion [i.e., the neutral (N) and desialylated acidics] were separated by Bio-Gel P-4 (~400 mesh) gel permeation chromatography, and individual fractions were pooled as indicated (Figure 4b). The structures present within each oligosaccharide fraction (Figure 5) were determined by a combination of sequential exoglycosidase digestion, methylation analysis (of dextran-free material), and partial acetolysis. Assignment of glycosyl residue sequence, anomeric configuration of individual glycosidic linkages, and in some cases the position of glycosyl linkages is based on a consideration of the specificities of the exoglycosidases and the changes in hydrodynamic volume of digested oligosaccharides (Yamashita et al., 1982). The sensitivity of each oligosaccharide fraction exposed to exoglycosidases in the order shown in Figure 5, and the change

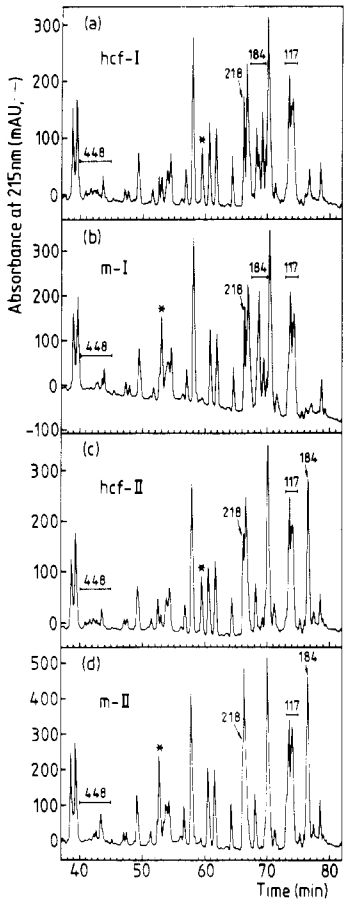

FIGURE 3: Reversed-phase HPLC of tryptic peptides from type I hcf-t-PA (a), type II hcf-t-PA (c), type I m-t-PA (b), and type II m-t-PA (d). Hcf-t-PA (approximately 330 μg of type I and 380 μg of type II) and m-t-PA (approximately 470 μg of type I and 600 μg of type II) were reduced, carboxymethylated, and digested with trypsin. Only the relevant portion of each chromatogram is shown. The elution positions of peptides containing the potential N-glycosylation sites Asn-117, Asn-184, Asn-218, and Asn-448 are indicated. The C-terminal A-chain peptide, QYSQPQF (hcf-t-PA) or QYSQPQFR (m-t-PA), is also indicated (*).

in hydrodynamic volume effected by each exoglycosidase treatment [as judged by Bio-Gel P-4 (~400 mesh) gel permation chromatography], is consistent with the structures shown. The methylation analysis (Table IV) establishes the position(s) at which glycosyl residues are substituted in each oligosaccharide fraction (except h-A where insufficient material was available) and provides structural information not always available from the results of exoglycosidase digestion. Finally, localization of outer arm substitutions to either the Manα1→6 or Manα1→3 arm is achieved by controlled acetolysis of the enzymatically defucosylated oligosaccharide fraction under conditions such that the only detectable hydrolysis is that of the Manα1→6 linkage (see Materials and Methods), together, in some cases, with sequential exoglycosidase digestion of the (reduced) product (Table V). In all cases where both controlled acetolysis and jack bean α-mannosidase digestion under arm-specific conditions (see Materials and Methods) were used, the results obtained were in agreement.

For oligosaccharide pools found to contain two or more different structures, the relative incidence of each was determined after products, diagnostic of each individual structure, had been generated by a sequence of exoglycosidase digestions, and separated by Bio-Gel P-4 (~400 mesh) gel permeation chromatography. As an illustrative example, consider oligosaccharide fraction h-G. As judged by its peak shape in the Bio-Gel P-4 (~400 mesh) gel permeation chromatogram of the desialylated oligosaccharides (Figure 4b), h-G clearly consists of at least two different oligosaccharides. Incubation of fraction h-G with the *A. phoenicis* α1→2-specific mannosidase, followed by separation of the products by Bio-Gel P-4 (~400 mesh) gel permeation chromatography, generates a product eluting at 8.9 g.u. (indicating a loss of two α1→2 mannose residues) and a peak centered around 11.2 g.u. (unaffected). The 8.9 g.u. product was resistant to all exoglycosidases except jack bean α-mannosidase, which converted it to a product eluting at 5.5 g.u. This 5.5 g.u. product was initially susceptible only to *A. fulica* β-mannosidase, and then to jack bean β-*N*-acetylhexosaminidase. This sequence of

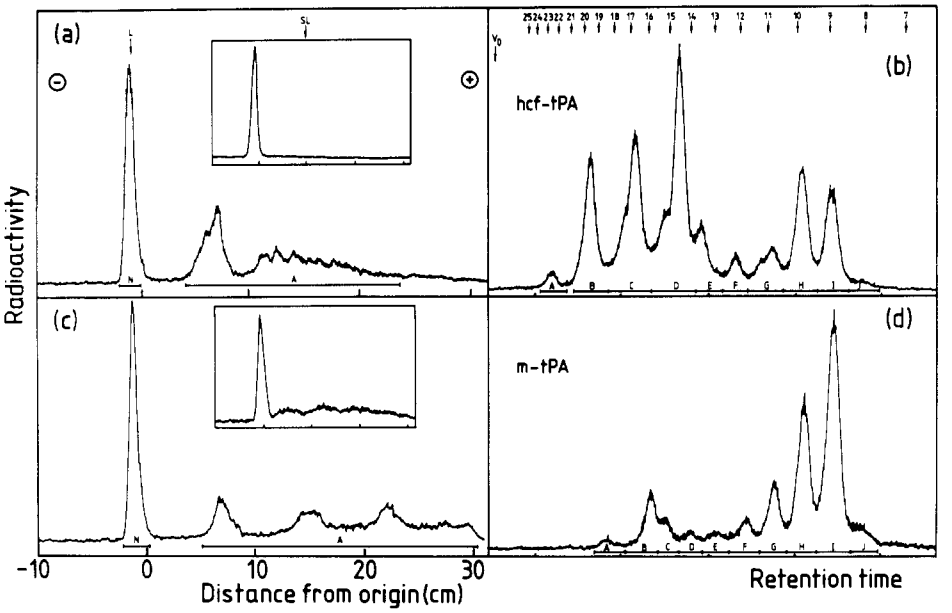

FIGURE 4: High-voltage radioelectrophoretograms (a, c) and Bio-Gel P-4 (~400 mesh) gel permeation chromatograms (b, d) of the oligosaccharides derived from hcf-t-PA (a, b) and m-t-PA (c, d). Insets (a, c) are of the high-voltage radioelectrophoretograms of the oligosaccharides after exhaustive neuraminidase digestion. Following separation of the desialylated oligosaccharides by Bio-Gel P-4 (~400 mesh) gel permeation chromatography, individual fractions were pooled as indicated (b, d) for further analysis. Neutral (N) and acidic (A) oligosaccharides (a, c) were recovered by elution with water. L = lactitol; SL = 3′(6′)-sialyllactitol.

Table III: Relative Incidence and Site Distribution of Neutral, Sialylated, Sulfated, and Complex-, Hybrid-, and Oligomannose-Type Oligosaccharides of hcf-t-PA and of m-t-PA[a]

glycoprotein/glycopeptide	neutral (%)	sialylated (%)	sulfated (%)	complex (%)	hybrid[b] (%)	oligomannose (%)
hcf-t-PA (unfractionated)	53	47	nd[c]	65	7	28
hcf-t-PA ($\sum$ I and II)[d]	70	30	nd	59	9.5	31
hcf-I (intact)	79	21	nd	67	9	23
hcf-I ($\sum$ sites)[e]	85	15	nd	63	10	27
hcf-I Asn-117	>99	nd	nd	11	16	73
hcf-I Asn-184	81	19	nd	84	8	8
hcf-I Asn-448	74	26	nd	93	7	nd
hcf-II (intact)	61	39	nd	51	10	39
hcf-II ($\sum$ sites)[e]	65	35	nd	52	10	38
hcf-II Asn-117	>99	nd	nd	11	14	74
hcf-II Asn-448	31	69	nd	93	6	1
m-t-PA (unfractionated)	63	7	30	25	6	69
m-t-PA ($\sum$ I and II)[d]	72	4	25	28	7	65
m-I (intact)	91	7	2	30.5	4.5	65
m-I ($\sum$ sites)[e]	89	9	2	43	5	52
m-I Asn-117	>99	nd	nd	nd	nd	>99
m-I Asn-184	81	19	nd	60	8	32
m-I Asn-448	87	7	6	69	7	24
m-II (intact)	53	nd	47	26	9	65
m-II ($\sum$ sites)[e]	64	nd	36	37	4	58
m-II Asn-117	>99	nd	nd	nd	nd	>99
m-II Asn-448	28	nd	72	74	9	17

[a] The relative incidence in a given sample of glycoprotein or glycopeptide of neutral, sialylated, and sulfated oligosaccharides was determined as described in Table III and under Materials and Methods. The relative incidence of complex-, hybrid-, and oligomannose-type structures in each case was calculated from the results presented in Tables IV and VII, with assignment of an individual oligosaccharide structure to a particular class based on the structures shown in Figures 5 and 7. [b] Oligosacchairde h-G-1 has been deemed to be of the hybrid-type class. [c] nd = none detectable. [d] These values are calculated on the basis of the recoveries of type I and type II t-PA forms from the lysine–Sepharose chromatography separation (Materials and Methods and Figure 2). For both hcf-t-PA and m-t-PA the two forms were recovered in essentially equimolar amounts, based on protein recovery. [e] These values are calculated assuming complete glycosylation at each glycosylation site of type I and type II t-PA. The close agreement between the values calculated by summing the results of the site analysis and the experimentally determined value for the intact glycoprotein confirms this assumption and establishes the accuracy of this analysis.

Table IV: Methylation Analysis of the Desialylated Oligosaccharides Released from Unfractionated hcf-t-PA[a]

		oligosaccharide fraction								
methylated monosaccharide	linkage	h-B	h-C	h-D	h-E	h-F	h-G	h-H	h-I	h-J
fucitol										
2,3,4-tri-*O*-methyl (1,5-di-*O*-acetyl)	t[b]	+[c]	+	+	–[c]	–	+	–	–	–
galactitol										
2,3,4,6-tetra-*O*-methyl (1,5-di-*O*-acetyl)	t	+	+	+	+	+	+	–	–	–
mannitol										
2,3,4,6-tetra-*O*-methyl (1,5-di-*O*-acetyl)	t	–	–	–	–	+	+	+	+	+
3,4,6-tri-*O*-methyl (1,2,5-tri-*O*-acetyl)	2	–	+	+	+	+	+	+	–	–
2,4,6-tri-*O*-methyl (1,3,5-tri-*O*-acetyl)	3	–	–	–	–	–	+	–		+
2,3,4-tri-*O*-methyl (1,5,6-tri-*O*-acetyl)	6	–	–	–	–	–	+	–	–	+
3,6-di-*O*-methyl (1,2,4,5-tetra-*O*-acetyl)	2,4	+	+	–	–	–	–	–	–	–
3,4-di-*O*-methyl (1,2,5,6-tetra-*O*-acetyl)	2,6	+	+	+	–	–	–	–	–	–
2,4-di-*O*-methyl (1,3,5,6-tetra-*O*-acetyl)	3,6	+	+	+	+	+	+	+	+	+
2-(*N*-methylacetamido)-2-deoxyglucitol										
3,4,6-tri-*O*-methyl (1,5-di-*O*-acetyl)	t	–	–	+	–	–	–	–	–	–
3,6-di-*O*-methyl (1,4,5-tri-*O*-acetyl)	4	+	+	+	+	+	+	+	+	+
1,3,5,6-tetra-*O*-methyl (4-mono-*O*-acetyl)	4OL	–	+	–	+	+	+	+	+	+
1,3,5-tri-*O*-methyl (4,6-di-*O*-acetyl)	4,6OL	+	+	+	–	–	+	–	–	–

[a] Oligosaccharides were released from unfractionated hcf-t-PA and reduced as described (Materials and Methods). Following separation of desialylated oligosaccharides by Bio-Gel P-40 (~400 mesh) gel permeation chromatography (dextran free), individual fractions were separately pooled (see Figure 4b) and methylation analysis was performed as described (Materials and Methods). Insufficient material was available for analysis of fraction h-A. [b] t = terminal. [c] (+) designates presence and (–) the absence of the partially methylated alditol acetate in the relevant fraction.

exoglycosidase digestions suggests that one of the structures (h-G-3 in Figure 5) present within the oligosaccharide fraction h-G is "Man 7". The 11.2 g.u. peak (unaffected by *A. phoenicis* α1→2-specific mannosidase) was converted by incubation with jack bean β-galactosidase to a product of elution volume 10.2 g.u. (indicating a loss of one β1→4 galactose residue), and this product was then converted to one of 8.2 g.u. by *S. pneumoniae* β-N-acetylhexosaminidase (indicating the loss of one β1→2GlcNAc residue). This 8.2 g.u. product was incubated with jack bean α-mannosidase, and two products were formed, one eluting at 6.5 g.u. and one at 5.5 g.u. This indicates that the 8.2 g.u. product consisted of two structures, one with three α-linked mannose residues, and the other with two. Both the 6.5 g.u. and the 5.5 g.u. products were susceptible to *A. fulica* β-mannosidase, then to jack bean β-N-acetylhexosaminidase, and, in the case of the 6.5 g.u. product, also to bovine epididymis α-fucosidase. Hence, oligosaccharide pool h-G consists of three different structures. The results obtained from these exoglycosidase digestions and the methylation analysis (Table IV) of oligosaccharide pool h-G are consistent with the proposed structures h-G-1, h-G-2, and h-G-3, as shown in Figure 5. Additional evidence in support of the structures shown comes from partial acetolysis of pool h-G after enzymatic defucosylation (Table V). The absence of a product at 6.5 g.u. after partial acetolysis confirms that in h-G-2 it is only the Manα1→3 arm that carries outer arm substitutions. The products that are generated (at 7.5 g.u. and between 9.7 and 9.1 g.u.) do not allow such a conclusion

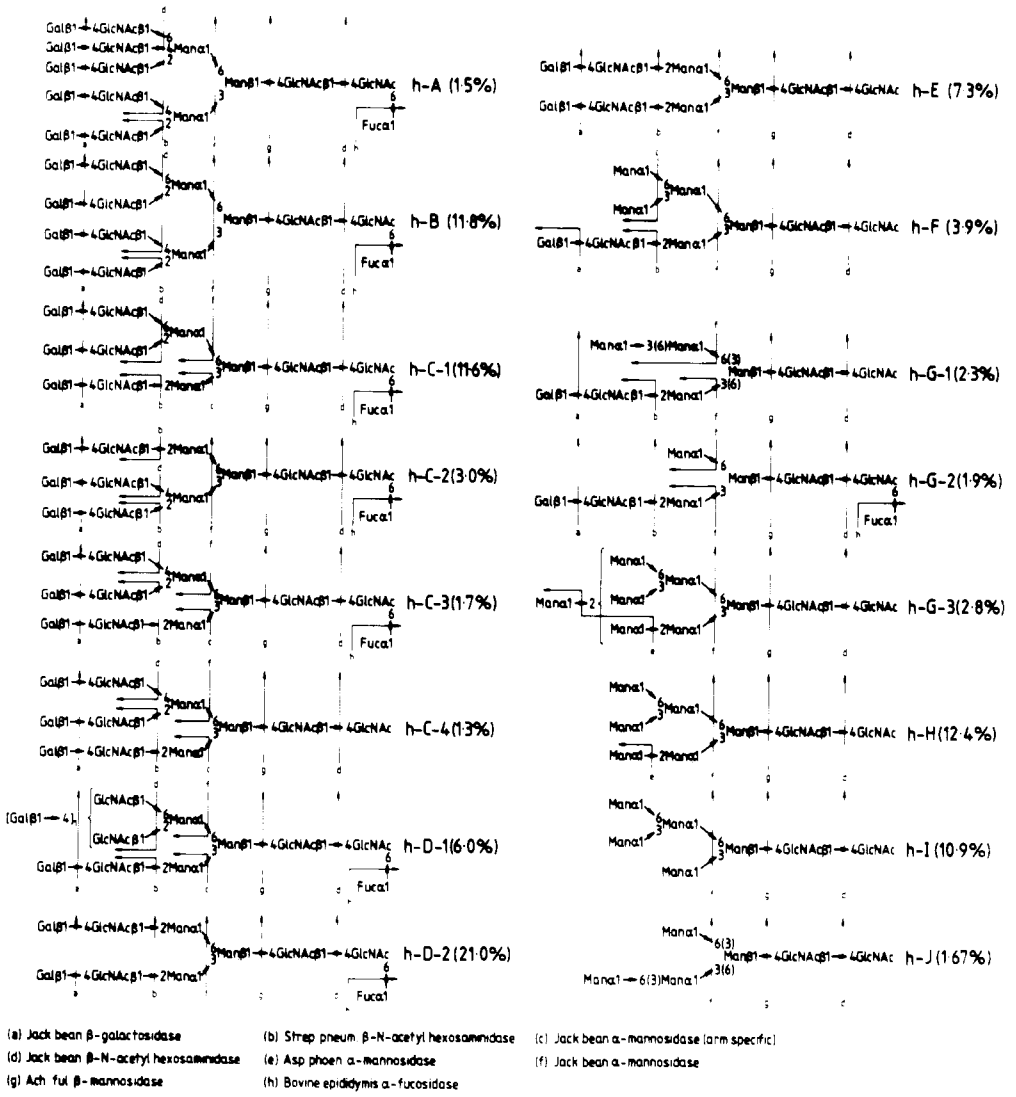

FIGURE 5: Structures of the neutral and desialylated N-linked oligosaccharides derived from unfractionated hcf-t-PA. Structural analysis was performed on individual oligosaccharide fractions (Figure 4b) by using a combination of sequential exoglycosidase digestion [using the exoglycosidases indicated and with separation of the products by Bio-Gel P-4 (~400 mesh) gel permeation chromatography], methylation analysis (on dextran-free material), and partial acetolysis, all as described under Materials and Methods. Changes in the hydrodynamic volume of oligosaccharide structures were effected by exoglycosidases when used in the following order: oligosaccharide h-A, a-b-d-f-g-d-h; oligosaccharide h-B, a-b-d-f-g-d-h; oligosaccharide h-C-1, a-b-c-d-f-g-d-h; oligosaccharide h-C-2, a-b-d-f-g-d-h; oligosaccharide h-C-3, a-b-c-d-f-g-d-h; oligosaccharide h-C-4, a-b-c-d-f-g-d; oligosaccharide h-D-1, a-b-c-d-f-g-d-h; oligosaccharide h-D-2, a-b-f-g-d-h; oligosaccharide h-E, a-b-f-g-d; oligosaccharide h-F, c-a-b-f-g-d; oligosaccharide h-G-1, a-b-f-g-d; oligosaccharide h-G-2, a-b-f-g-d-h; oligosaccharide h-G-3, e-f-g-d; oligosaccharide h-H, e-f-g-d; oligosaccharide h-I, f-g-d; oligosaccharide h-J, f-g-d. The deduced points of hydrolysis of each structure by individual exoglycosidases are indicated, together with the relative incidence of each structure in the desialylated oligosaccharide pool. Where linkage positions could not be unequivocally established, all possible structures are shown.

concerning h-G-1 but are consistent with those predicted for the structures h-G-1, h-G-2, and h-G-3, as shown. Hence, it is concluded that the oligosaccharide fraction h-G consists of the three structures shown in Figure 5. All the other oligosaccharide fractions were analyzed in a similar way.

Structural Analysis of the N-Linked Oligosaccharides Released from Unfractionated m-t-PA. An aliquot of the mixture of reduced oligosaccharides isolated from unfractionated m-t-PA was first subjected to high-voltage paper electrophoresis, and the resulting profile is shown in Figure 4c. The relative amount of neutral (N) and acidic components was calculated from the relative recovery of radioactivity from the relevant regions of the paper (Table III). Treatment of these acidic oligosaccharides with Newcastle disease virus neuraminidase caused no conversion of these to neural oligosaccharides (data not shown), but treatment with *A. ureafaciens* neuraminidase did, as judged by analysis of the products by high-voltage paper electrophoresis (Figure 4c, inset). This indicates that $\alpha 2 \rightarrow 6$-linked sialic acid is present within the acidic structures. That other acidic groups are also present is indicated by the incomplete conversion to neutral structures after neuraminidase treatment (Figue 4c, inset). The neuraminidase-resistant oligosaccharides were also resistant to cold aqueous HF (0 °C, 50% v/v, 30 h) but were completely converted to neutral oligosaccharides by methanolic HCl (Figure 6). It is therefore concluded that these oligosaccharides did not contain phosphate groups but were rendered acidic by the presence of one or more sulfate groups (McCarthy & Baker, 1979). The relative content of acidic oligosaccharides that were only sialylated and those that were either only sulfated or both sulfated and sialylated was calculated after recovery of radioactivity from the relevant regions of the paper. The neutral (N) and desialylated nonsulfated oligosaccharides were pooled and fractionated by Bio-Gel P-4 (~400 mesh) gel permeation chromatography, and individual fractions were pooled as indicated in Figure 4d. The structures present within each oligosaccharide fraction were determined by a combination of sequential exoglycosidase digestion, methylation analysis (of dextran-free material), and partial acetolysis. The results, presented in Figure 7 and Tables V and VI, are consistent with the structures proposed in Figure 7. In the case of the desulfated oligosaccharides, fractionation

Table V: Results of Partial Acetolysis on Individual Oligosaccharide Fractions Obtained by Bio-Gel P-4 (~400 Mesh) Gel Permeation Chromatography of the Desialylated Oligosaccharide Pool Derived from hcf-t-PA and m-t-PA[a]

oligosaccharide fraction	elution vol postdefucosylation (g.u.)	elution vol of product(s) after partial acetolysis (g.u.)
h-A	21.5	12.3[b]
h-B	18.5	12.3[b]
h-C	16.2	12.3[b] and 9.3[b]
h-D	14.2 and 13.3	9.3[b]
h-E	13.3	9.3[b]
h-F	12.2	11.3[b] and 9.3[b]
h-G	11.5–10.1	9.7–9.1 and 7.5
h-H	9.9	9.3 and 7.5
h-I	8.9	8.3 and 6.5
m-B	15.1	11.6[c]
m-C	15.2 and 14.2	11.6[c] and 10.3[c]
m-D	14.1 and 13.1	10.3[c]
m-E	13.0	12.5 and 11.6[c]
m-F	11.8–11.3	10.3 and 8.5
m-G	10.5	9.3 and 7.5
m-H	9.9	9.3 and 7.5
m-I	8.9	8.3 and 6.5

[a] Individual oligosaccharide fractions were defucosylated and subjected to partial acetolysis as described under Materials and Methods. The products of acetolysis were separated by Bio-Gel P-4 (~400 mesh) gel permeation chromatography, and only the radioactive products (retaining the original reduced terminus) were detected. The elution volume of this (these) product(s) is given in the third column. Fractions h-J, m-A, and m-J were not analyzed. For a discusson of the use of acetolysis on complex sugars, see Elices and Goldstein (1989). [b] After degalactosylation with jack bean β-galactosidase, this product was susceptible to *S. pneumoniae* β-*N*-acetylhexosaminidase. [c] This product was resistant to *S. pneumoniae* β-*N*-acetylhexosaminidase but was converted to one eluting at 6.5 g.u. by jack bean β-*N*-acetylhexosaminidase.

by Bio-Gel P-4 (~400 mesh) gel permeation chromatography generated the profile shown in Figure 6c. This material is currently under investigation.

Analysis of the N-Glycosylation of Purified Type I and Type II hcf- and m-t-PA, and of Each N-Glycosylation Site Derived Therefrom. The reduced oligosaccharides recovered from each glycoprotein, or pool of glycopeptides derived from each N-glycosylation site, were first analyzed with respect to the relative incidence of neutral, sialylated, and sulfated oligosaccharide species, as already described. These results are summarized in Table III. Following incubation with neuraminidase, the neutral and desialylated oligosaccharides were fractionated by Bio-Gel P-4 (~400 mesh) gel permeation chromatography (see Figure 8 for intact type I and type II t-PA and Figure 9 for each N-glycosylation site). In the case of oligosaccharide fractions known (from analysis of unfractionated m- and hcf-t-PA) to contain more than one oligosaccharide (i.e., h-C, h-D, h-G, m-C, m-D, and m-F), the relative incidence of each individual structure was determined after sequential exoglycosidase analysis of the oligosaccharide fraction. These results are summarized in Tables VII and VIII.

Accuracy of the Analysis. In any analysis of this nature, it is essential to determine whether fractionation of a glycoprotein or isolation of glycopeptides is in any way selective with respect to oligosaccharide, i.e., whether the relative recoveries of individual glycopeptides or glycoprotein forms are equivalent or not.

In Table III is presented a comparison between the *experimentally* determined relative incidence of each oligosaccharide "characteristic" of a glycoprotein and the relative incidence of each such "characteristic" as calculated from the experimentally determined values for each type of t-PA or pool of glycopeptides, i.e., a comparison between the glycosylation

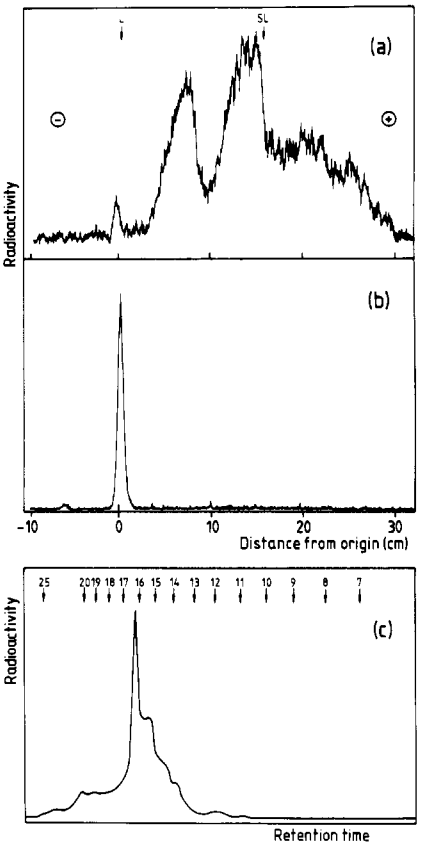

FIGURE 6: Analysis of the neuraminidase-resistant acidic oligosaccharides derived from m-t-PA. Oligosaccharides were subjected to high-voltage paper electrophoresis (see Materials and Methods) after exhaustive digestion with neuraminidase (a) and after methanolysis (b). The radioactive oligosaccharides remaining at the origin after methanolysis were recovered and subjected to Bio-Gel P-4 (~400 mesh) gel permeation chromatography (c).

of the intact glycoprotein and the "reconstituted" one. In all cases, the experimentally determined and calculated values are in close agreement. This indicates that separation of unfractionated t-PA into type I and type II was not associated with any selective loss of oligosaccharide and also that isolation of the glycopeptides from individual N-glycosylation sites of type I and type II t-PA was likewise nonselective. While this comparison does not rule out the possibility of an oligosaccharide influence on isolation of the unfractionated t-PA, it does indicate that the type and site analysis reported here is highly accurate.

Reconstruction of Composite Glycoforms of hcf-t-PA and of m-t-PA. Within a given type of hcf- and m-t-PA, certain N-glycosylation sites are occupied by more than one class of oligosaccharide and, further, each N-glycosylation site is unique with respect to the relative incidence at that site of each class of oligosaccharide, and of each acidic group (i.e., sialic acid or sulfate), as shown in Table III. Both hcf- and m-t-PA will therefore consist of different glycoforms or molecules differing with respect to the structure and disposition of oligosaccharides on a common polypeptide (Parekh et al., 1987). Using the site-analysis data summarized in Table III, it is possible to reconstruct "composite" glycoforms for each form of t-PA (Figure 10). Each composite glycoform would itself consist of a set of discrete glycoforms, each of which carries different oligosaccharides of the same type at a given N-glycosylation site.

Discussion

Most of the structures presented in this study have previously been reported on glycoproteins derived from human or

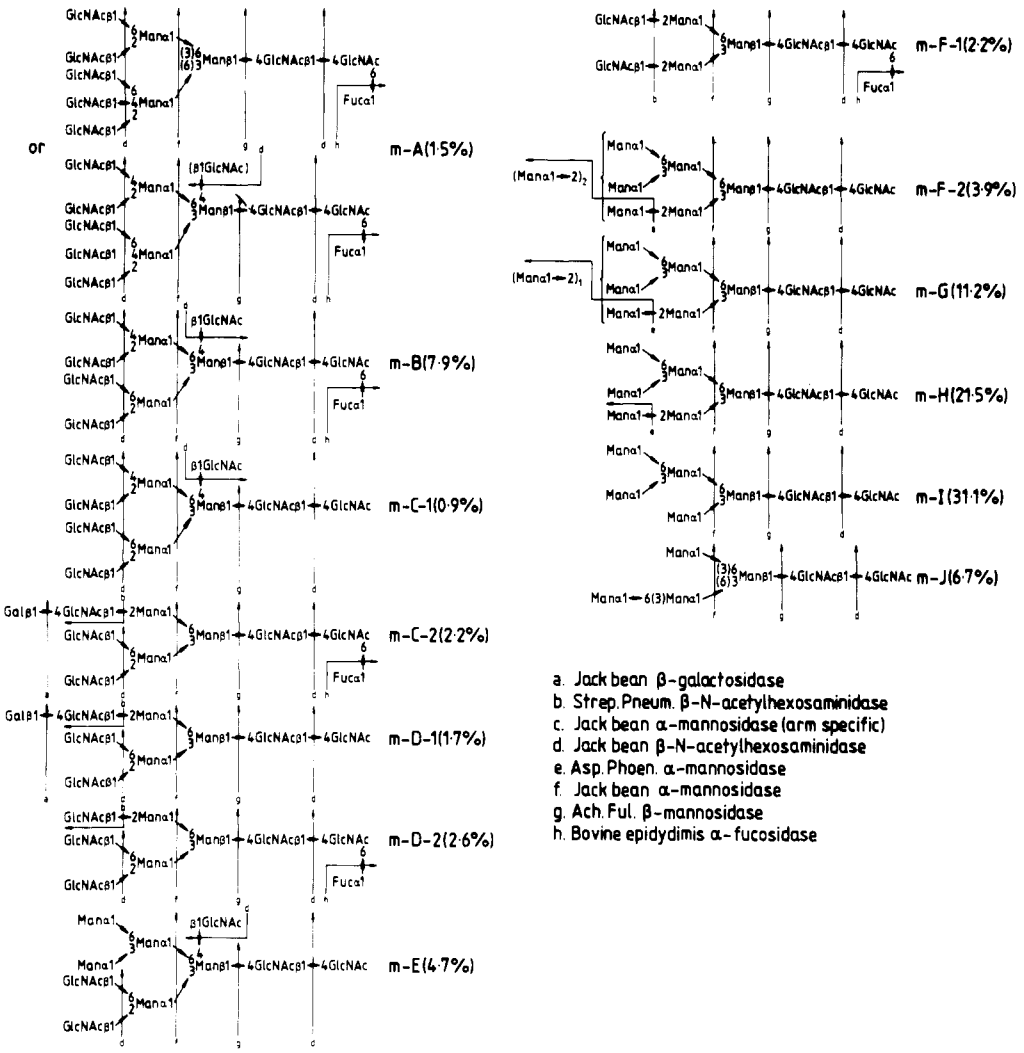

FIGURE 7: Structures of the neutral and desialylated N-linked oligosaccharides derived from unfractionated m-t-PA. Structural analysis was performed on individual oligosaccharide fractions (Figure 4d) by using a combination of sequential exoglycosidase digestion [using the exoglycosidases indicated and with separation of the products by Bio-Gel P-4 (~400 mesh) gel permeation chromatography], methylation analysis (on dextran-free material), and partial acetolysis, all as described under Materials and Methods. Changes in the hydrodynamic volume of oligosaccharide structures were effected by exoglycosidases when used in the following order: oligosaccharide m-A, d-f-g-d-h; oligosaccharide m-B, d-f-g-d-h; oligosaccharide m-C-1, d-f-g-d; oligosaccharide m-C-2, a-b-d-f-g-d-h; oligosaccharide m-D-1, a-b-d-f-g-d; oligosaccharide m-D-2, b-d-f-g-d-h; oligosaccharide m-E, d-f-g-d; oligosaccharide m-F-1, b-f-g-d-h; oligosaccharide m-F-2, e-f-g-d; oligosaccharide m-G, e-f-g-d; oligosaccharide m-H, e-f-g-d; oligosaccharide m-I, f-g-d; oligosaccharide m-J, f-g-d. The deduced points of hydrolysis of each structure by individual, exoglycosidases are indicated, together with the relative incidence of each structure in the desialylated oligosaccharide pool. Where linkage positions could not be unequivocally established, all possible structures are shown.

Table VI: Methylation Analysis of the Desialylated Oligosaccharides Released from Unfractionated m-t-PA[a]

methylated monosaccharide	linkage	oligosaccharide fraction							
		m-B	m-D	m-E	m-F	m-G	m-H	m-I	m-J
fucitol									
2,3,4-tri-*O*-methyl (1,5-di-*O*-acetyl)	t[b]	+[c]	+	–[c]	–	–	–	–	–
galactitol									
2,3,4,6-tetra-*O*-methyl (1,5-di-*O*-acetyl)	t	–	+	–	–	–	–	–	–
mannitol									
2,3,4,6-tetra-*O*-methyl (1,5-di-*O*-acetyl)	t	–	–	+	+	+	+	+	+
3,4,6-tri-*O*-methyl (1,2,5-tri-*O*-acetyl)	2	–	+	–	+	+	+	–	–
3,6-di-*O*-methyl (1,2,4,5-tetra-*O*-acetyl)	2,4	+	–	–	–	–	–	–	–
3,4-di-*O*-methyl (1,2,5,6-tetra-*O*-acetyl)	2,6	+	+	+	–	–	–	–	–
2,4-di-*O*-methyl (1,3,5,6-tetra-*O*-acetyl)	3,6	–	+	+	+	+	+	+	+
2-mono-*O*-methyl (1,3,4,5,6-penta-*O*-acetyl)	3,4,6	+	–	+	–	–	–	–	–
2-(*N*-methylacetamido)-2-deoxyglucitol									
3,4,6-tri-*O*-methyl (1,5-di-*O*-acetyl)	t	+	+	+	+	–	–	–	–
3,6-di-*O*-methyl (1,4,5-tri-*O*-acetyl)	4	+	+	+	+	+	+	+	+
1,3,5,6-tetra-*O*-methyl (4-mono-*O*-acetyl)	4OL	–	+	+	+	+	+	+	+
1,3,5-tri-*O*-methyl (4,6-di-*O*-acetyl)	4,6OL	+	+	–	+	–	–	–	–

[a] Oligosaccharides were released from unfractionated m-t-PA and reduced as described (Materials and Methods). Following separation of desialylated oligosaccharides by Bio-Gel P-4 (~400 mesh) gel permeation chromatography (dextran free), individual fractions were separately pooled (see Figure 4c) and methylation analysis was performed as described (Materials and Methods). Insufficient material was available for analysis on fraction m-A and m-C. [b] t = terminal. [c] (+) designates presence and (–) the absence of the partially methylated alditol acetate in the relevant fraction.

Table VII: Relative Incidence and Site Distribution of the Individual Desialylated Oligosaccharides of hcf-t-PA[a]

oligo-saccharide	hcf-t-PA (unfractionated)	hcf-I				hcf-II		
		intact	Asn-117	Asn-184	Asn-448	intact	Asn-117	Asn-448
h-A	1.3[b]	2.4	nd[c]	nd	2.4	1.8	nd	2.0
h-B	11.6	8.5	nd	3.6	19.1	10.2	nd	20.3
h-C-1	11.4	11.6	nd	11.1	18.3	9.8	nd	21.2
h-C-2	2.9	3.4	nd	3.2	5.4	3.3	nd	8.0
h-C-3	1.5	1.6	nd	2.0	2.2	0.9	nd	3.1
h-C-4	1.2	1.5	nd	1.6	1.1	1.0	nd	2.4
h-D-1	5.8	4.8	0.7	12.4	9.9	3.0	0.8	5.0
h-D-2	20.3	17.3	3.2	39.3	24.2	8.6	2.2	18.8
h-E	7.4	13.3	6.0	8.6	8.0	9.0	4.6	11.2
h-F	4.2	5.9	10.2	4.3	3.3	4.9	10.0	3.8
h-G-1	2.6	3.4	5.4	3.6	4.1	5.5	4.3	2.4
h-G-2	2.2	3.1	1.7	2.3	1.9	2.7	3.7	1.1
h-G-3	2.7	3.5	12.0	0.7	0.3	4.9	12.6	0.7
h-H	12.7	9.0	31.0	2.8	nd	17.7	29.1	nd
h-I	10.7	8.1	22.6	4.4	nd	14.0	23.2	nd
h-J	1.5	2.7	7.2	nd	nd	2.6	9.5	nd

[a] The desialylated oligosaccharides derived from an individual glycoprotein or glycopeptide of hcf-t-PA were separated by Bio-Gel P-4 (~400 mesh) gel permeation chromatography and the fractions pooled as indicated in Figure 4b. In the case of pools h-C, h-D, and h-G, the relative incidence of individual oligosaccharides present within each pool was determined by sequential exoglycosidase digestion (Materials and Methods and Figure 5). [b] The hcf-t-PA preparation used for isolation of type I and type II hcf-t-PA was different from that used for the structural analysis of the hcf-t-PA-associated oligosaccharides (Figure 5). Both preparations were obtained in the same way from cultures of the same cell line, and the P-4 profiles of the desialylated oligosaccharides derived from them were very similar. For this reason, the relative incidence of the individual fractions in the unfractionated hcf-t-PA in this table is very close to, but not identical with, that reported in Figure 5. [c] nd = none detectable.

Table VIII: Relative Incidence and Site Distribution of the Individual Desialylated Oligosaccharides of m-t-PA[a]

oligosaccharide	m-t-PA (unfractionated)	m-I				m-II		
		intact	Asn-117	Asn-184	Asn-448	intact	Asn-117	Asn-448
m-A	1.8[b]	3.9	nd[c]	4.1	10.3	4.6	nd	11.4
m-B	11.8	12.1	nd	22.5	26.5	6.9	nd	28.1
m-C-1	1.2	1.8	nd	4.7	3.1	1.8	nd	4.8
m-C-2	2.4	4.3	nd	11.0	7.2	2.4	nd	7.8
m-D-1	1.9	2.3	nd	6.2	5.1	1.9	nd	5.9
m-D-2	3.1	3.9	nd	8.5	9.0	4.7	nd	10.2
m-E	5.7	4.5	nd	7.8	7.5	8.8	nd	8.5
m-F-1	2.4	2.2	nd	3.1	7.6	3.9	nd	6.2
m-F-2	4.5	9.7	11.4	10.1	2.3	9.9	11.8	1.7
m-G	12.1	15.4	23.7	7.5	7.0	14.7	22.8	3.5
m-H	20.6	19.1	34.1	7.7	5.4	18.2	33.9	6.5
m-I	25.9	16.2	25.7	6.8	5.3	14.4	26.1	5.4
m-J	5.9	4.6	5.1	nd	3.7	7.7	5.4	nd

[a] The desialylated oligosaccharides derived from an individual glycoprotein or glycopeptide of m-t-PA were separated by Bio-Gel P-4 (~400 mesh) gel permeation chromatography and the fractions pooled as indicated in Figure 4c. In the case of pools m-C, m-D, and m-F, the relative incidence of individual oligosaccharides present within each pool was determined by sequential exoglycosidase digestion (Materials and Methods and Figure 7). [b] The m-t-PA preparation used for isolation of type I and type II m-t-PA was different from that used for the structural analysis of the m-t-PA-associated oligosaccharides (Figure 7). Both preparations were purchased from American Diagnostica (see Materials and Methods), and the P-4 profiles of the oligosaccharides (neutral and desialylated) derived from them were very similar. For this reason, the relative incidence of the individual fractions in the unfractionated m-t-PA in this table is very close to, but not identical with, that reported in Figure 7. [c] nd = none detectable.

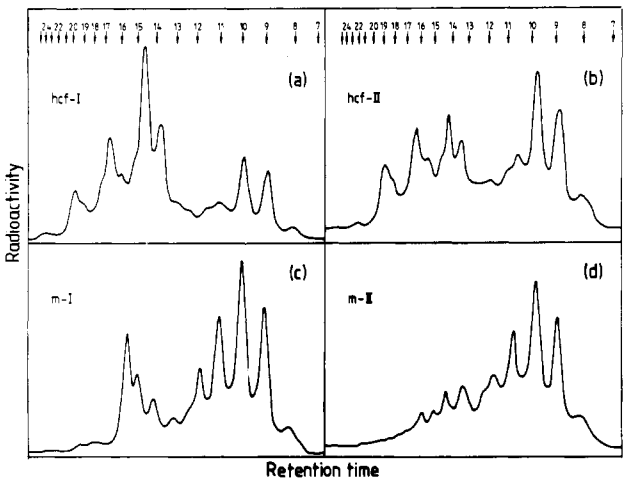

FIGURE 8: Bio-Gel P-4 (~400 mesh) gel permeation chromatograms of the desialylated oligosaccharides derived from hcf-t-PA types I (a) and II (b) and m-t-PA types I (c) and II (d).

other species (Yamashita et al., 1982; Kobata, 1984). The structural analysis on the N-linked oligosaccharides associated with the Bowes melanoma derived t-PA is in general agreement with the methylation analysis reported by Pohl et al. (1987), but several differences should be noted. The first concerns the incidence of tri-, tetra-, and pentaantennary oligosaccharides in the glycopeptides derived from Asn-184. The methylation analysis of Pohl et al. (1987) suggests an absence of such structures from this site, whereas our results indicate a relative incidence of 25.7%, 27.2%, and 4.1%, respectively. Further, we detect oligomannose structures at this site (~32%) while Pohl et al. (1987) detect none. Of particular interest is the detection by Pohl et al. of a partially methylated monosaccharide consistent with a 3,4-di-O-substituted *N*-acetylglucosamine residue in the N-linked oligosaccharides derived from Asn-448. While this could indicate the occurrence of Fucα1→3(Galβ1→4)GlcNAcβ1→, as suggested by Pohl et al. (1987), we find no evidence for such an outer arm substitution during our structural analysis of the desialylated oligosaccharides. However, 3,4-di-O-substituted *N*-acetylglucosamine may be present in the sulfated oligosaccharides (located exclusively at Asn-448), which were not subjected to structural analysis in this study.

The analysis reported here on the N-glycosylation of a single polypeptide expressed in two cell types of the same species

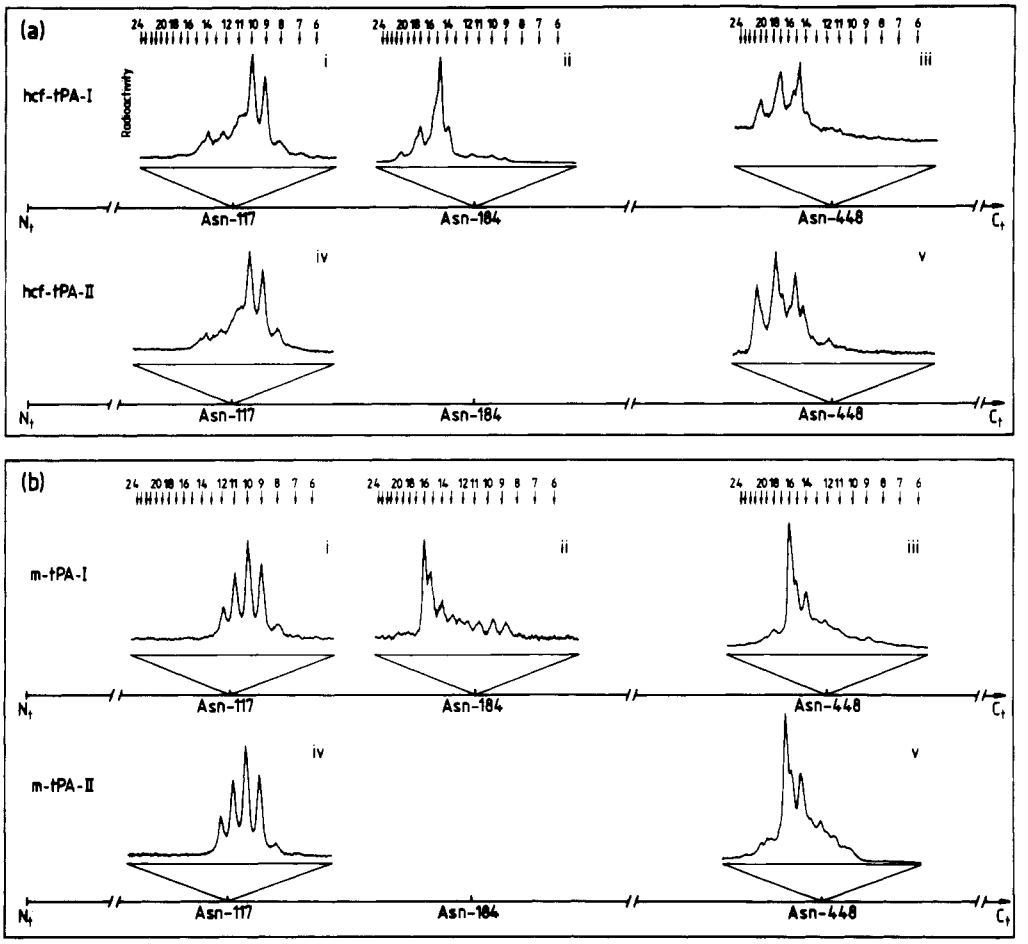

FIGURE 9: Bio-Gel P-4 (~400 mesh) gel permeation chromatograms of the desialylated oligosaccharides derived from each N-glycosylated site of hcf-t-PA types I (ai, ii, iii) and II (aiv, v) and m-t-PA types I (bi, ii, iii) and II (biv, v).

sheds further light on the factors controlling N-glycosylation. As judged by the final set of structures associated with hcf-t-PA and m-t-PA (Figures 5 and 7), there are both qualitative and quantitative differences between hcf cells and Bowes melanoma cells with respect to their expression of glycosyltransferase activities (i.e., each has an unique *glycotype*). For example, the melanoma, but not hcf, cells appear to express GnT III and GnT VII and a sulfotransferase. Conversely, the hcf cells express GnT IV, an activity not expressed in melanoma cells (Schachter et al., 1983). The origin of these qualitative differences is not known. The range of ecto- and exocellular glycosyltransferases reported to date is inconsistent with the idea that these differences arise from differential processing after secretion of a common precursor. The hcf cell strain is derived from normal colon tissue, and the Bowes melanoma cell line is polyploid and lacks no chromosomes. While qualitative differences in genetic content between the two cell types cannot be formally excluded, it is considered unlikely that these account for the qualitative differences in glycosyltransferase expression between the two cell types. It is more likely that these differences arise from differential control of gene expression, differences in intracellular localization of these enzymes, or differences in the intracellular route taken by the t-PA polypeptide. Quantitative differences in N-glycosylation between the two cell types are also evident, particularly with respect to the activities of *N*-acetylglucosaminyltransferases, GnT V, and GnT VI. The origin of these differences is likewise currently a matter of conjecture, and it cannot be stated whether it is due principally to the transformed state or to natural differences in N-glycosylation capacity between fibroblasts and melanocytes.

Numerous studies have indicated that the polypeptide can exert an influence on its N-glycosylation (Trimble et al., 1983; Hsieh et al., 1983; Yet et al., 1988), and the results presented here provide further support for this idea. The analysis of oligosaccharide structures present at each of the various N-glycosylation sites, summarized in Tables III, IV, and VII and in Figure 9, clearly indicates site-specific N-glycosylation. In hcf-t-PA (both types I and II), Asn-117 is associated predominantly with oligomannose structures, while the structures at Asn-184 (likewise located in a Kringle domain) and Asn-448 are much more highly processed, being associated essentially only with complex structures. In m-t-PA, the structures at Asn-117 are exclusively oligomannose, while at Asn-184 and Asn-448 the structures are more highly processed. In both cell types, therefore, the oligosaccharides at Asn-117 remain largely unprocessed compared with the structures at Asn-184 and Asn-448. This situation is reminiscent of the N-glycosylation of rat Thy-1 from brain and thymocytes (Parekh et al., 1987), where structures at the first N-glycosylation site (Asn-23) in both tissues are largely unprocessed compared to those at the two subsequent sites (namely, Asn-74 and Asn-98). It is interesting to note that some structures (27%) at Asn-117 in hcf-t-PA are acted upon by GnT I (Schachter et al., 1983), whereas essentially none is at Asn-117 in m-t-PA. Yet GnT I is expressed by melanoma cells, as judged by its high activity on oligosaccharides at Asn-184 and Asn-448 in m-t-PA.

The molecular basis for site-specific N-glycosylation is not known, but it is generally argued that the polypeptide environment around an N-golycosylation site in *some* cases constrains the action of the N-glycosylation apparatus [for a discussion, see Yet et al. (1988)]. Various mechanisms have been proposed to account for this. For example, direct effects of polypeptide on oligosaccharide conformation through polypeptide–oligosaccharide interactions have been invoked in the case of IgG (Savvidou et al., 1984) and through steric

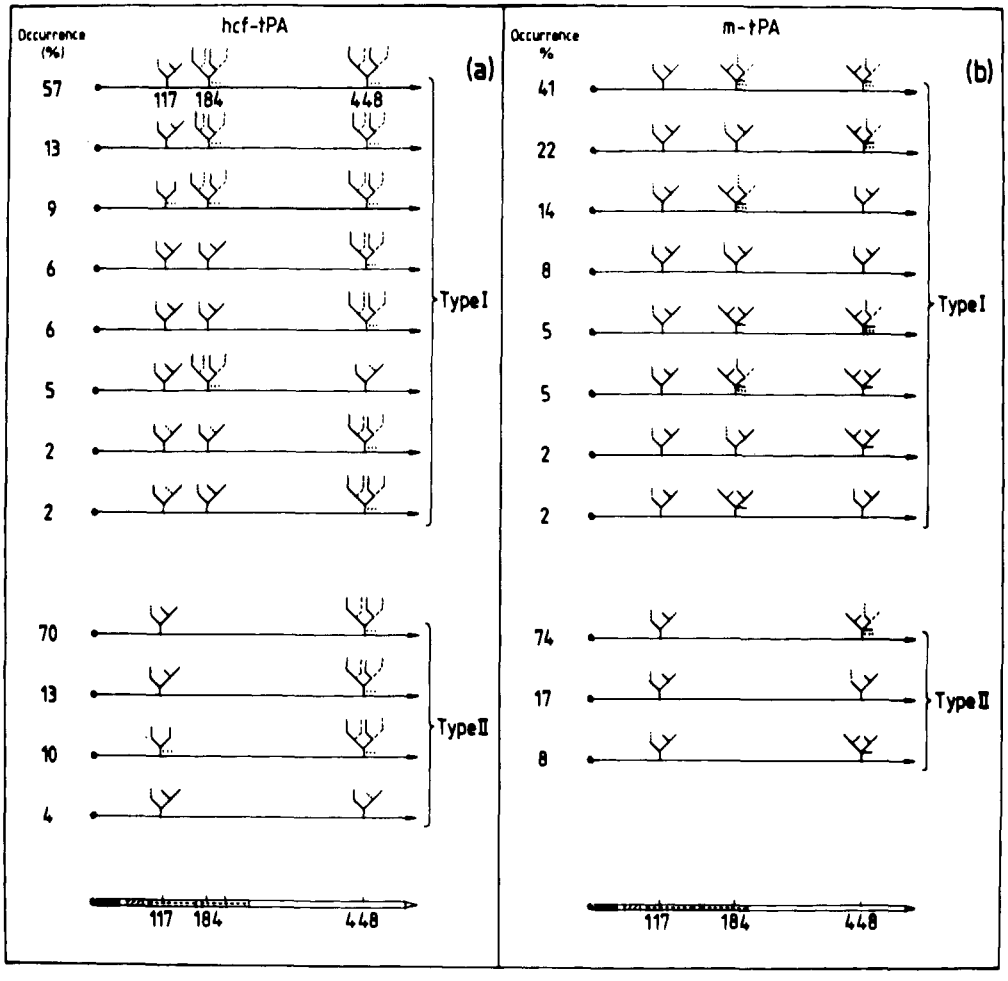

FIGURE 10: "Composite" glycoforms found in hcf- and m-t-PA. The occurrence of each composite glycoform was calculated from the analysis of N-glycosylation at each individual site (Table IX), assuming that such N-glycosylation was independent of that at other sites. The Manα1→3Manβ→R branch is drawn to the left, and the Manα1→6Manβ→R branch is drawn to the right (see below). The location of N-glycosylation sites and regions of homology with other polypeptides are indicated as described in the legend to Figure 1. Symbols represent the following:

Manα1→3Manβ→R branch to the left and Manα1→6Manβ→R branch to the right

biantennary oligosaccharides with some core fucosylation

Man-5 with Man-6

hybrid oligosaccharides with either Manα1→6(3) or Manα1→6(Manα1→3) on the Manα1→6 arm

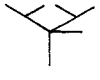

hybrid oligosaccharides with a "bisecting" GlcNAc and GlcNAcβ1→2(GlcNAcβ1→6) on the Manα1→3 arm and Manα1→6(Manα1→3) on the Manα1→6 arm

core-fucosylated bi- and triantennary oligosaccharides with a trace of tetraanntennary oligosaccharides

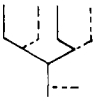

core-fucosylated bi-, tri-, and tetraantennary oligosaccharides

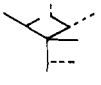

triantennary oligosaccharides with 2,6-linked branching on the Manα1→3 arm, core fucosylation, and a "bisecting" GlcNAc, with some outer arm galactosylation of the Manα1→6 arm, tetraantennary oligosaccharides (2,4-linked branching on the Manα1→6 arm and 2,6-linked branching on the Manα1→3 arm) with no outer arm galactosylation, and a trace of biantennary oligosaccharides

control of accessibility in the case of yeast carboxypeptidase (Trimble et al., 1983). Indirect effects, through an influence on intracellular routing, may be responsible for the unique N-glycosylation of lysosomal enzymes (Kornfeld, 1985). Any mechanism to explain the restriction on processing of oligosaccharide structures at Asn-117 in t-PA must take account of the following two facts. First, the relative size of the N-linked oligosaccharides when compared to the Kringle domain (a model to scale of these is shown in Figure 11); and second, oligosaccharides at Asn-184 in Kringle K2 can be fully processed, while those at Asn-117 in Kringle K1 cannot. The relative size of the oligosaccharides makes it unlikely that the local polypeptide microenvironment around an N-glycosylation site can so dramatically influence oligosaccharide processing at the relatively far-removed nonreducing termini of the oligosaccharide. Rather, the polypeptide may exert its influence over a much greater distance, consistent with the recently reported effects of quaternary structure on oligosaccharide processing (Dahms & Hart, 1986). This may explain how such large oligosaccharides, attached to two presumably structurally homologous domains, can be processed so differently depending on their precise point of attachment to that domain. Alternatively, the Kringle domain may possess an oligosaccharide-binding site which can be occupied by oligosaccharides attached at Asn-117 (thus restricting their processing), but not by those at Asn-184. The idea that some effects of polypeptide on oligosaccharide processing are through distal rather than proximal interactions is relevant to the approach of genetic deletion in localizing a function to a particular polypeptide domain. A change in function of a recombinant polypeptide after deletion of a defined nucleotide coding segment could arise from alterations in oligosaccharide processing, and such an effect could occur over a considerable distance.

A comparison of the processing of oligosaccharides at Asn-117 in type I and type II t-PA from either hcf or melanoma cells (Figure 9) shows that this site is N-glycosylated in an essentially identical manner in both type I and type II t-PA. This is also the case for oligosaccharides at Asn-448 of hcf-t-PA. Hence, N-glycosylation at Asn-184 cannot have any significant effect on the processing of oligosaccharides at Asn-117 and Asn-448 in hcf-t-PA. In the case of m-t-PA, N-glycosylation at Asn-184 clearly does not affect processing of oligosaccharides at Asn-117 but may influence the activity of certain processing enzymes on structures at Asn-448, since Asn-448 carries sulfated oligosaccharides in type II but not in type I m-t-PA.

As in the case of other secreted glycoproteins which similarly exist in variant forms differing with respect to the degree of N-glycosylation, the mechanistic basis for the partial occupancy of the sequon Asn-184 is not known. The similarity between type I and type II t-PA with respect to N-glycosylation at other sites (Figure 9), while not constituting definitive proof, would argue for a common cellular origin of both forms. If so, it would suggest that the polypeptide around Asn-184 may only transiently be in a suitable conformation for Asn-184 to be a substrate for the oligosaccharyltransferase, and then the relative amounts of type I and type II t-PA produced by a cell would reflect a balance between the activity of oligosaccharyltransferase and the kinetics of folding of the polypeptide around Asn-184. If this model is true, it suggests that the type I and type II t-PA polypeptides differ with respect to conformation, at least around Asn-184. Alternatively, interaction of some polypeptides with BiP (binding protein) in the endoplasmic reticulum may influence the overall degree of N-glycosylation (Dorner et al., 1987). It must also be considered that glycosylation of Asn-184 is contingent upon early processing events at Asn-117.

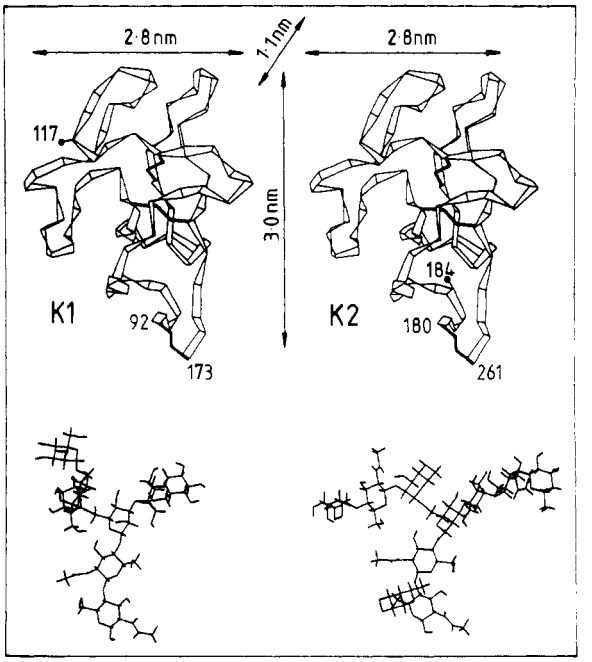

FIGURE 11: A comparison of the relative sizes of the two Kringle domains (K1 and K2) and the Man-5 oligosaccharide (located at Asn-117 of K1 and shown below K1) and the desialylated biantennary oligosaccharide with core fucose (located at Asn-184 of K2 and shown below K2). The Kringle structures are taken directly from the X-ray crystallographic study of bovine prothrombin fragment 1 (Park & Tulinsky, 1986). No adjustments have been made for amino acid deletions, substitutions, and additions, when compared to the homologous t-PA structures. The conservation of amino acid residues necessary for the Kringle fold (Park & Tulinsky, 1986) suggests that the t-PA Kringles will be similar to those of bovine prothrombin fragment 1, shown here. Residues in the Kringle structure of prothrombin that correspond to the Cys-92–Cys-173 (K1) and Cys-180–Cys-261 (K2) disulfide bridges of t-PA are indicated, as are the residues homologous to Asn-117 and Asn-184 of t-PA. The three-dimensional carbohydrate structures were generated by combining the component di- and trisaccharides of each carbohydrate, and the dihedral angles were calculated by using the parametrized molecular orbital package AMPAC. The complete carbohydrate structure has not been minimized.

Despite similarities with respect to the degree of processing of the structures at individual N-glycosylation sites, Bowes melanoma and hcf cells do not produce any glycoforms in common (Figure 10). This was also the case for rat Thy-1 isolated from brain and thymocytes (Parekh et al., 1987). An effect of the combination of a unique cellular glycotype, the influence of polypeptide structure on oligosaccharide processing, and the combinatorial association of oligosaccharides at different glycosylation sites on a polypeptide may be to create a set of glycoforms of that polypeptide which is unique to the cellular population that expresses it. That is, the structure and spatial disposition of oligosaccharides on a polypeptide may constitute an exquisitely specific statement of cellular origin. In Figure 11, two of the N-linked oligosaccharides on hcf-t-PA and the Kringle polypeptide domain of bovine prothrombin (Park & Tulinsky, 1986) have been modeled to scale. In view of the considerable size of the oligosaccharides in relation to the polypeptide, the potential for diversifying a polypeptide, both structurally and functionally, through modulation of the degree and nature of N-glycosylation is clearly immense. While in no case has biochemical separation of all glycoforms of a polypeptide yet been achieved, there is increasing evidence that different glycoforms can differ with respect to structure and function (Malaise et al., 1987). In the case of t-PA, expressed by Bowes melanoma and hcf cells, such differences have been detected,

and these are discussed in a subsequent report.

The range of glycoforms of a polypeptide expressed by a single cell type raises interesting questions with respect to glycoform biosynthesis. For example, does each cell within the population express all glycoforms, a unique subset, or just one? Should the N-glycosylation of one polypeptide change under external influences, is there a similar and concomitant change in the N-glycosylation of *all* the other glycoproteins being expressed by the cellular population in question? If not, how is such a change avoided? Why do such changes in the N-glycosylation of a polypeptide not lead to immune rejection? Perhaps an organism simultaneously expresses all the glycoforms of a polypeptide that it will ever be required to express, and controls the relative *levels* of each at any given time. In this regard it is interesting to note the controlled changes in the levels of human IgG glycoforms that occur during pregnancy (G. A. W. Rook, A. Whyte, J. Steele, R., Brealey, P. Arkwright, C. Redman, R. A. D. Dwek, P. Williams and T. W. Rademacher, unpublished results) and the subsequent aging of the individual (Parekh et al., 1988).

Finally, these results have significant implications for the genetic engineering of mammalian glycoproteins, including t-PA. Expression of the desired polypeptide in recombinant form in a cell type in which it is not normally expressed would probably lead to the production of a nonphysiological set of glycoforms. Irrespective of changes in any functions of that glycoprotein which are normally mediated directly by oligosaccharide, these glycoforms may have unusual additional properties arising from novel N-glycosylation. These may include new circulatory properties, changes in tropism, and immunogenicity (Rademacher et al., 1988). Clearly, a choice of cell-expression system during production of recombinant glycoproteins must include a comparison of the glycotype of the cell in question and the ultimate recipient of that recombinant glycoprotein.

ACKNOWLEDGMENTS

We are grateful to Dr. Jitka Olander for providing the monoclonal antibody to t-PA (clone 79-7), to Dr. C. J. Edge for modeling the three-dimensional structures of the oligosaccharides shown in Figure 11, and to B. Matthews, P. M. Rudd, K. Levinson, A. Robinson, B. Young, and L. Patton for technical assistance. The Oxford Glycobiology Unit is supported by the Monsanto Co., and G.O. is a senior research assistant of the Belgian National Fund for Scientific Research (NFWO) and was sponsored in part by the General Savings and Retirement Fund (ASLK Belgium).

REFERENCES

Astrup, T., & Permin, P. H. (1947) *Nature 159*, 681–682.
Bachmann, F., & Kruithof, E. K. O. (1984) *Semin. Thromb. Hemostasis 10*, 6–17.
Banyai, L., Varadi, A., & Patthy, L. (1983) *FEBS Lett. 163*, 37–41.
Bischoff, J., Liscum, L., & Kornfield, R. (1986) *J. Biol. Chem. 261*, 4766–4774.
Bok, R. A., & Mangel, W. F. (1985) *Biochemistry 24*, 3279–3286.
Ciucanu, I., & Kerek, F. (1987) *Carbohydr. Res. 131*, 209–217.
Collen, D., Rijken, D. C., Van Damme, J., & Billiau, A. (1982) *Thromb. Haemostasis, 48*, 294–296.
Dahms, N. M., & Hart, G. W. (1986) *J. Biol. Chem. 261*, 13186–13196.
Dorner, A. J., Bole, D. G., & Kaufman, R. J. (1987) *J. Cell Biol. 105*, 2665–2674.
Einarsson, M., Brandt, J., & Kaplan, L. (1985) *Biochim. Biophys. Acta 830*, 1–10.
Elbein, A. D. (1987) *Annu. Rev. Biochem. 56*, 497–534.
Elices, M.J., & Goldstein, I. J. (1989) *J. Biol. Chem. 264*, 1375–1380.
Glasgow, L. R., Paulson, J. C., & Hill, R. L. (1977) *J. Biol. Chem. 252*, 8615–8623.
Harakas, N. K., Schasumann, J. P., Connolly, D. T., Wittwer, A. J., Olander, J. V., & Feder, J. (1988) *Biotechnol. Prog.* (in press).
Hayes, M. L., & Castellino, F. J. (1979) *J. Biol. Chem. 254*, 8768–8771.
Hsieh, P., Rosner, M. R., & Robbins, P. W. (1983) *J. Biol. Chem. 258*, 2555–2561.
Hunkapiller, M. W., Hedwick, R. M., Dreyer, R. J., & Hood, L. E. (1983) *Methods Enzymol. 91*, 399–413.
Ichishima, E., Arai, M., Shigematsu, Y., Kumagai, H., & Sumida-Tanaka, R. (1981) *Biochim. Biophys. Acta 658*, 45–53.
Jany, K. D., Keil, W., Meyer, H., & Kiltz, H. H. (1976) *Biochim. Biophys. Acta 453*, 62–66.
Kobata, A. (1979) *Anal. Biochem. 100*, 1–14.
Kobata, A. (1984) in *Biology of Carbohydrates* (Ginsburg, V., & Robbins, P. W., Eds.) pp 87–162, John Wiley and Sons, New York.
Kornfeld, R., & Kornfeld, S. (1985) *Annu. Rev. Biochem. 54*, 631–664.
Kornfeld, S. (1985) *J. Clin. Invest. 77*, 1–6.
Kruithof, E. K. O., Schleuning, W.-D., & Bachmann, F. (1985) *Biochem. J. 226*, 631–636.
Li, Y. T., and Li, S. C. (1972) *Methods Enzymol. 28*, 702–713.
Little, S. P., Band, N. U., Harms, C. S., Marks, C. A., & Mattler, L. E. (1984) *Biochemistry 23*, 6191–6195.
Malaise, M. G., Franchimont, P., Gornez, F., Bouilleno, C., & Mahieu, P. R. (1987) *Clin. Immunol. Immunopathol. 45*, 1–16.
McCarthy, M. M. U., and Baker, J. R., (1979) *Carbohydr. Res. 69*, 151–164.
Mullins, D. E., & Rohrlich, S. T. (1983) *Biochim. Biophys. Acta 695*, 177–214.
Natsuka, S., Hase, S., & Ikenaka, T. (1987) *Anal. Biochem. 167*, 154–159.
Opdenakker, G., Van Damme, J., Bosman, F., Billiau, A., & De Somer, P. (1986) *Proc. Soc. Exp. Biol. Med. 182*, 248–257.
Parekh, R. B., Tse, A. G. D., Dwek, R. A., Williams, A. F., & Rademacher, T. W. (1987) *EMBO J. 6*, 1233–1244.
Parekh, R., Roitt, I., Isenberg, D., Dwek, R., & Rademacher, T. (1988) *J. Exp. Med. 167*, 1731–1736.
Park, C. H., & Tulinsky, A. (1986) *Biochemistry 25*, 3977–3982.
Paulson, J. C., Weinstein, J., Dorland, L., van Halbeek, H., & Vliegenthart, J. F. G. (1982) *J. Biol. Chem. 257*, 12734–12738.
Pennica, D., Holmes, W. E., Kohr, W. J., Harkins, R. N., Vehar, G. A., Ward, C. A., et al. (1983) *Nature 301*, 214–221.
Pohl, G., Kallstrom, M., Bergsdorf, N., Wallen, P., & Jornvall, H. (1984) *Biochemistry 23*, 3701–3707.
Pohl, G., Kenne, L., Nilsson, B., & Einarsson, M. (1987) *Eur. J. Biochem. 170*, 69–75.
Rademacher, T. W., Parekh, R. B., & Dwek, R. A. (1988) *Annu. Rev. Biochem. 57*, 785–838.
Ranby, M. (1982) *Biochim. Biophys. Acta 704*, 461–469.
Ranby, M., Bergsdorf, N., Pohl, G., & Wallen, P. (1982)

FEBS Lett. 146, 289-292.
Reich, E. (1975) in *Proteases and Biological Control* (Reich, E., Rifkin, D. B., & Shaw, E., Eds.) pp 333-341, Cold Spring Harbor Laboratory, Cold Spring Harbor, NY.
Rijken, D. C., & Collen, D. (1981) *J. Biol. Chem. 256*, 7035-7041.
Rijken, D. C., Eneis, J. J., & Gerwig, G. J. (1985) *Thromb. Haemostasis 54(4)*, 788-791.
Savvidou, G., Klein, M., Grey, A. A., Dorrington, K. J., & Carver, J. P. (1984) *Biochemistry 23*, 3736-3740.
Schachter, H., Narasinhan, S., Gleeson, P., & Vella, G. (1983) *Can. J. Biochem. Cell Biol. 61*, 1049-1066.
Thorsen, S., Glas-Greenwalt, P., & Astrup, T. (1972) *Thromb. Diath. Haemorrh. 28*, 65-74.
Trimble, R. B., Maley, F., & Chu, F. K. (1983) *J. Biol. Chem. 258*, 2562-2567.
Verstraete, M., Bory, M., Collen, D., Erbel, R., Lennane, R. T., Mathey, D., et al. (1985) *Lancet April 13*, 842-847.
Wallen, P., Pohl, G., Bergsdorf, N., Ranby, M., Ny, T., & Jornvall, H. (1983) *Eur. J. Biochem. 132*, 681-686.
Yamashita, K., Mizuochi, T., & Kobata, A. (1982) *Methods Enzymol. 83*, 105-126.
Yet, M.-G., Shao, M.-C., & Wold, F. (1988) *FASEB J. 2*, 22-31.
Zamarron, C., Lijnen, H. R., & Collen, D. (1984) *J. Biol. Chem. 259*, 2080-2083.

Effects of N-Glycosylation on in Vitro Activity of Bowes Melanoma and Human Colon Fibroblast Derived Tissue Plasminogen Activator

Arthur J. Wittwer, Susan C. Howard, Linda S. Carr, Nikos K. Harakas, and Joseph Feder*
Department of Cell Culture and Biochemistry, Monsanto Company, St. Louis, Missouri 63167
Raj B. Parekh, Pauline M. Rudd, Raymond A. Dwek, and Thomas W. Rademacher*,‡
Glycobiology Unit, Department of Biochemistry, University of Oxford, South Parks Road, Oxford OX1 3QU, U.K.
Received September 30, 1988; Revised Manuscript Received May 2, 1989

ABSTRACT: Tissue-type plasminogen activator (t-PA), when isolated from human colon fibroblast (hcf) cells, is N-glycosylated differently than when isolated from the Bowes melanoma (m) cell line (Parekh et al., 1988). Both hcf- and m-t-PA can be separated into type I t-PA (with three occupied N-glycosylation sequons, at Asn-117, -184, and -448) and type II t-PA (with two occupied sequons, at Asn-117 and -448). Oligosaccharide analysis of each of these types of t-PA indicates that hcf-t-PA and m-t-PA have no glycoforms in common, despite having the same primary amino acid sequence. We have therefore compared in vitro the enzymatic activities and fibrin binding of type I and type II hcf- and m-t-PA with those of aglycosyl t-PA isolated from tunicamycin-treated cells. Plasminogen activation kinetics were determined by using an indirect amidolytic assay with Glu-plasminogen and a chromogenic plasmin substrate. In the absence of stimulator, there was little difference in activity between type I and type II t-PA, but the activity of aglycosyl t-PA was 2-4-fold higher than that of the corresponding glycosylated t-PA. In the presence of a fibrinogen fragment stimulator, the K_{cat} value of type II t-PA was approximately 5-fold that of type I t-PA from the same cell line, while the K_m values for activation of Glu-plasminogen were similar (0.13-0.18 μM). The stimulated activity of glycosyl t-PA was similar to that of type II t-PA. No effect of glycosylation was seen when each t-PA was assayed directly with H-D-Val-Gly-Arg-*p*-nitroanilide. In a clot lysis assay, type II t-PA was 23-26% more active than the type I t-PA from the same cell line, while type I and type II m-t-PA were about 30% more active, respectively, than type I and type II hcf-t-PA. The fibrin binding ability of each t-PA correlated very well with clot lysis activity but not with the stimulated indirect amidolytic activity. Together, these results suggest that sequon occupancy of Asn-184 (in addition to Asn-117 and -448) significantly decreases the fibrin-dependent stimulation of t-PA activity. Occupancy of sequons Asn-117 and -448 decreases the unstimulated activity of t-PA, and the nature of the oligosaccharide at Asn-448 influences both fibrin binding and clot lysis activity.

Human t-PA[1] is a glycoprotein containing four potential N-glycosylation sites (Pennica et al., 1983). In type I t-PA, only three of these are occupied, and in type II t-PA, only two are occupied (Pohl et al., 1984). We have recently defined in detail the N-glycosylation of t-PA derived from a human colon fibroblast (hcf) cell strain and a Bowes melanoma (m) cell line (Parekh et al., 1989). In both these cases it was shown that N-glycosylation served to create a number of variants (*glycoforms*) of the t-PA polypeptide and that there were no common glycoforms between the t-PA derived from the two cell lines, and hence the t-PA from these two cell lines are chemically distinct. We now assess some of the effects of these defined differences in N-glycosylation on the specific activity

* Authors to whom correspondence should be addressed.
‡ Author to whom reprint requests should be addressed.

[1] Abbreviations: t-PA, tissue-type plasminogen activator; hcf, human colon fibroblast; m, Bowes melanoma; mAU, milli absorbance units; ELISA, enzyme-linked immunosorbent assay; SDS-PAGE, gel electrophoresis in the presence of sodium dodecyl sulfate; DMEM, Dulbecco's modified Eagle's medium.

0006-2960/89/0428-7662$01.50/0